Cuffless Calibration and Estimation of Continuous Arterial Blood Pressure

GU, Wenbo

A Thesis Submitted in Partial Fulfillment of the Requirements for the Degree of Master of Philosophy

in

Electronic Engineering

The Chinese University of Hong Kong

September 2009


香港中文大學
大學
圖書館系統
15 FEB 2011
UNIVERSITY
LIBRARY SYSTEM
THE CHINESE UNIVERSITY OF HONG KONG

Acknowledgment

First of all, I would like to express my deep gratitude to my supervisor Prof. Yuan-Ting Zhang for encouraging me in various ways to complete my research study for the degree of master of philosophy. He is an energetic and strict researcher with amazing insight and countless creative ideas. I've really learned a lot from working with him. Moreover, I would like to thank him for introducing me into the academic area of biomedical engineering, which is exciting and promising with various attractive topics.

I would also like to appreciate my colleague in the Joint Research Center for Biomedical Engineering. My special thanks go to Ms. Carmen Chung Yan Poon for her lasting support and valuable suggestions on my research work. Warmest thanks also go to Ms. Iris Yan, Ms. Yin-Bo Liu, Ms. Qing Liu, Ms. Yan Li, Ms. Xiao-Fei Teng, Ms. Mico Wong, Ms. Jill Meng, Ms. Dan Wu, Ms. Ze Zhao, Ms. Linda Wang, Mr. Yong-Pei Liang, Mr. Fei Chen, Mr. Stanley Sy, Mr. Beli Lueng, Mr. Alex Wong, and Mr. Sheng-Yang Huang.

Finally, I would like to dedicate this thesis to my dearest mother and father. Their deepest love makes me so strong to meet any kinds of challenges in my life.

Abstract

Long term and continuous blood pressure (BP) measurements, especially those monitored at home, have been confirmed by many studies to provide better predictors of cardiovascular risk than those measured in conventional clinical settings. Three influential medical societies, the American Heart Association, American Society of Hypertension, and Preventive Cardiovascular Nurses Association, jointly made a scientific statement in 2008 to call to action on the use of home BP monitoring. However, existing non-invasive BP measurement technologies, e.g. the auscultative, oscillometric, tonometric or volume-clamp methods, have several drawbacks such as requirement of the use of an inflatable cuff, and therefore are bulky and uncomfortable for this purpose of measurement, especially in mobile or sleeping environment.

In contrast, the BP estimation based on pulse arrival time (PAT) is a promising way to meet the demand of long term and continuous BP monitoring without a bulky cuff. Only small, light and non-invasive transducers are needed for PAT measurement so that the device will be portable and comfortable. Thus BP can be estimated without inflatable cuffs and arterial occlusions by using the quasi-linear relationship between PAT and BP.

A main challenge of PAT-BP estimation is that the coefficients in PAT-BP equation have to be calibrated individually. Different calibration approaches have been proposed, amongst them, using one set of cuff BP readings is commonly considered. Nevertheless, the inclusion of cuff limits the miniaturization of equipment, and conflicts the purpose of "cuffless". Therefore, this research tries to investigate the possibility to innovate a new calibration method without using an inflatable cuff.

Firstly, analysis based on hemodynamic model, experiences from practical calibration method, and information of arterial elasticity properties contained in PPG waveform are studied, by which a new PAT-BP equation has been established. A novel cuffless calibration method based on this equation and PPG waveform analysis has been proposed while a cuff-based one is derived in the same way as a backup choice.

Secondly, experiments which lasted over months and included exercise procedures were conducted on a total of thirty-three subjects to evaluate this new cuffless calibration approach. Experiment results have proved that this calibration method is efficient for young subjects in sitting position, keeping a comparative accuracy than other cuffless calibration method, where no extra signal sensors are needed. Nevertheless, this approach may not be suitable for uses in supine position.

Thirdly, experiments including exercise were conducted on forty subjects, both young and aged groups, to investigate PAT-BP relationship in supine position. The substitute cuff-based calibration method has shown the potential in improving the PAT-BP estimation in this posture. The results have also indicated that factors such as age and posture changes should be considered carefully in BP estimation by PAT.

Moreover, a wearable device made as a shirt and a contactless system designed on a cushion were tested and evaluated during the experiments above. These novel systems show the attractive future of 24-hour PAT-BP monitoring whilst the daily activities and sleep of the user would not be disturbed at all.

In summary, research in this thesis not only covers the fundamental work, such as theoretical model-based analysis and the proposal of a novel cuffless calibration method, but also includes practical experiment verification and novel device evaluation for the long term and continuous cuffless arterial BP estimation.

摘要

大量科學研究證明，相比於在醫院測量的袖帶式血壓，長期連續測量的血壓、尤其是在家庭中持續監測到的血壓，可以更好地預測患心血管疾病死亡率及心血管事件。爲此，三大極具影響力的醫學協會——美國心臟協會、美國高血壓協會以及預防心血管病護士協會于 2008 年發表聯合聲明，提出家庭血壓監測應成爲心血管疾病診斷的主要依據。然而，現有的非侵入式血壓監測技術，如聽診法、振盪法、壓力傳感法、容積恒定法等，均不符合長期連續血壓監測的要求。例如，常見的聽診法或振盪法，其所用的充氣式袖帶將大大增加儀器的體積和重量，同時給使用者帶來擠壓血管的不適感，尤其不適用於行動或者睡眠的情況。

用脈搏波傳輸時間進行血壓預測或可成爲長期連續監測的關鍵技術。 由於測量脈搏波傳輸時間的感測器簡單輕便、不需要袖帶，相應的儀器可以十分便攜舒適。同時，血壓與脈搏波傳輸時間之間存在著近似線性的關係，因此，不需要壓迫血管或者皮膚，就可獲得即時連續的血壓估測。

在脈搏波傳輸時間-血壓估測領域，目前存在的主要難題是如何對估測公式進行針對不同個體的校準。在現有各種校準方法中，使用袖帶式測量所得的血壓值是最爲廣泛接受的。然而，這種方法不僅限制了測量儀器的小型化，更與“無袖帶”測量的目標相違背。因此，本研究的主要目的是探索一種新的方法，以實現連續血壓估測和校準均不需要充氣式袖帶。

首先，本論文系統分析了血液動力學模型、總結了現有校準方法的經驗以及探

索了光電容積描記圖波形所包含的血管彈性資訊。在此基礎上，提出了一個新的脈搏波傳輸時間-血壓關係式。根據這一關係式，建立了一個新型無袖帶式校準方法，同時還給出一個以同一原理爲基礎的有袖帶式校準方法作爲候補選擇。

第二，本研究用一系列跨數月時間、包含運動過程的實驗驗證了這一無袖帶校準方式的可行性。 共三十五個志願者參加了上述實驗。實驗結果證明，當使用者採取坐姿測量時，通過本無袖帶方法的校準，血壓估測精度較好。而且，在不需要任何額外信號感測器的情況下，本方法仍比現有的其他無袖帶校準方式更爲準確。但在採取臥姿的情況下，本方法並不適用。

第三，爲了研究在臥姿時脈搏波傳輸時間與血壓的關係，四十位志願者（包括青年組和老年組）參加了另一系列的實驗。在這些實驗中，志願者以平臥姿勢進行騎自行車運動。實驗結果顯示，本研究提出的候補袖帶式校準可以有效提高採用臥姿時血壓估測的精確度。該結果還表明年齡和姿勢改變都是影響脈搏波傳輸時間估測血壓的重要因素。

此外，在上述這些實驗中，本研究還測試評估了新型的穿戴式血壓測量衫及非接觸式血壓測量床墊。在不影響使用者正常活動和睡眠的情況下，這些創新的測量系統使得二十四小時連續血壓監測成爲可能。

總而言之，本研究不僅涉及廣泛的理論模型研究和實驗經驗總結，爲脈搏波傳輸時間估測血壓提出了新的無袖帶校準方法，同時也包含了多個實驗論證和實際測量系統測試。

List of Figures

List of Tables

List of Abbreviations

(In alphabetical order)

AAMI	Association for the Advancement of Medical Instrumentation
BP	blood pressure
DBP	diastolic blood pressure
ECG	electrocardiogram
MBP	mean blood pressure
mmHg	millimeter of mercury
PAT	pulse arrival time
PEP	pre-ejection period
PP	pulse pressure
PPG	photoplethysmogram
PTT	pulse transit time
PWV	pulse wave velocity
RMSE	root-mean-square error
SBP	systolic blood pressure
SD	standard deviation

Contents

1. Introduction

1.1. Arterial blood pressure and its importance

Human cardiovascular system is comprised of heart, blood and blood vessels. It looks like a closed water circuit. The heart keeps contracting as an intermittent pump to force the blood flowing into elastic tubes, i.e. the blood vessels. The blood travels through vessels in the order of arteries, capillaries and veins. Then the blood comes back to the heart, starting a new circulatory journey.

There is a pressure named arterial blood pressure (BP) generated with the blood flow in arteries to counteract the elastic counterforce of arterial walls and the hydraulic resistance [1]. It is a very important physiological parameter to show whether the performance of cardiovascular system is healthy. Numberless studies have shown the roles of blood pressure for disease prevention and diagnosis. For example, blood pressure too high, i.e. hypertension, means the increasing risk of heart attacks, heart failure and strokes [2].

Values of blood pressure differ in different sites of the arterial tree and vary with the systolic and diastolic movements of heart cycles. Usually, the term BP refers to the pressure in major blood vessels, such as brachial or aortic pressure. Moreover, there are several types of blood pressure which are mostly concerned: the highest pressure in each heart period - systolic blood pressure (SBP), the lowest pressure - diastolic blood pressure (DBP), the averaged pressure - mean blood pressure (MBP) as well as the difference between SBP and DBP - pulse pressure (PP). The standard unit for blood pressure measurement is millimeter of mercury (mmHg). The normal blood pressure values, for example, can be stated as 120 over 80 mmHg, where 120 is the SBP reading and 80 is the DBP reading [3].

In conventional medical treatment, blood pressure is preferred to be achieved in clinic office by professional nurses. In most cases, these measurements are intermittent and casual so that only several snapshots can be taken for each patient. However, in fact, blood pressure fluctuates continuously in a 24-hour period according to the invasive pressure monitoring by aortic catheter, whose changes can be even as large as tens of millimeters of mercury within several minutes [4]. Its sensitivity to drug injection, neural activities and emotional changes brings a lot of physiological information about the patients. Therefore, in order to increase the accuracy of disease diagnosis, doctors and researchers have paid more attentions recently on long term and continuous blood pressure monitoring, especially for those monitored at home.

According to the research on 5295 untreated hypertensive patients during a median follow-up period of 8.4 years, E. Dolan etc. compared three kinds of long term blood pressure monitoring (during-daytime, during-nighttime and 24-hour monitoring) with walk-in measurements in clinic. They pointed out that the former three kinds of measurements were superior to clinic measurement in predicting cardiovascular mortality, and nighttime blood pressure was the most potent predictor of outcome (Fig. 1.1) [5]. Clement etc. tracked 1963 hypertensive patients in approximately 5 years and found that the 24-hour ambulatory SBP is a greater independent risk factor for a new cardiovascular event than office SBP (Fig. 1.2) [6]. Works of Y. Shintani et al have shown that ambulatory blood pressure levels and its variability were closely associated with carotid artery alteration and these parameters should be independent predictors of carotid artery alteration [7]. The morning blood pressure surge was also considered as a destabilizing factor for atherosclerotic plaque causing cardiovascular events, such as ischemic and hemorrhagic stroke [8]-[11].

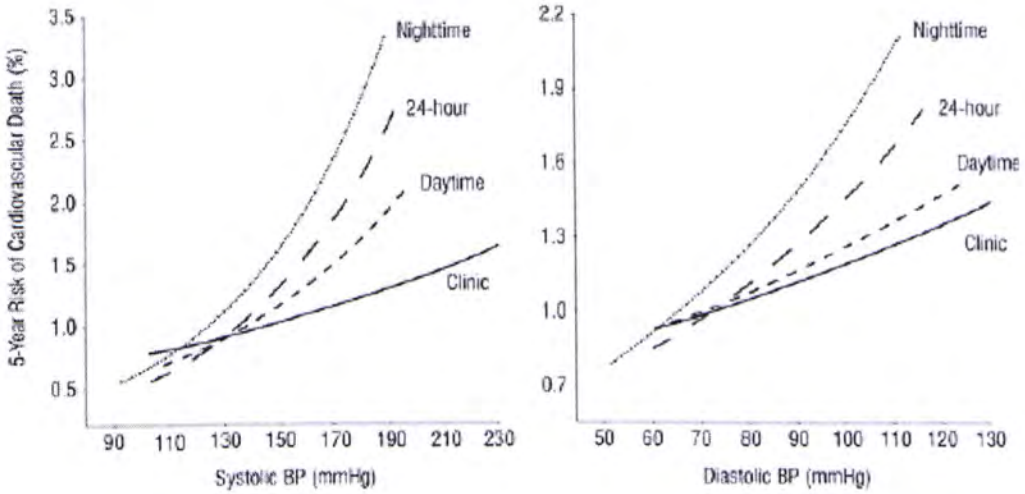

Fig. 1.1 Comparison of different types of blood pressure measurement: Adjusted 5-year risk of cardiovascular death in the study of 5929 patients [5]

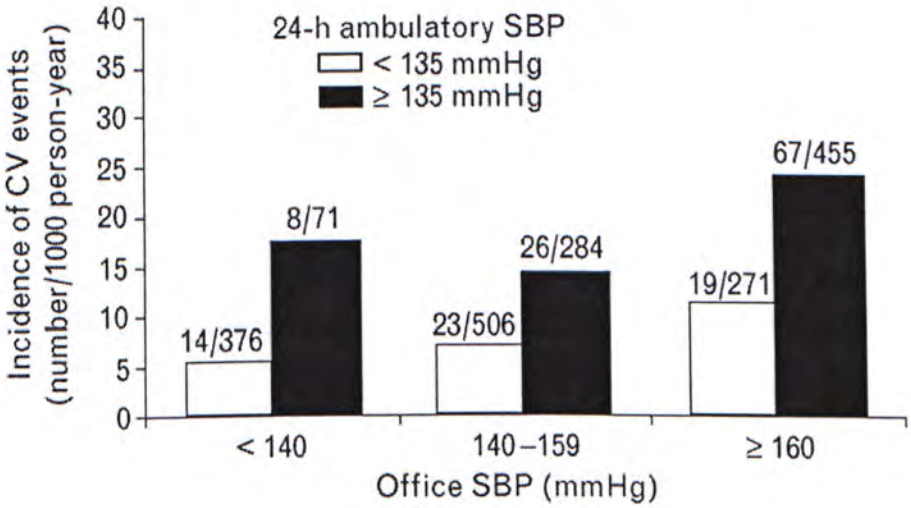

Fig. 1.2 High ambulatory systolic blood pressure (SBP≥135 mmHg) in hypertensive patients predicts cardiovasicular risk [6]

All these research results above show that long term blood pressure monitoring has performed better in predicting the cardiovascular diseases than the office measurement does. As the main and aimed part of long term monitoring, the importance of home blood pressure has been emphasized in a joint scientific statement in 2008 by three influential societies, the American Heart Association, American Society of Hypertension, and Preventive Cardiovascular Nurses Association [4]. Moreover, it is obvious that a continuous monitoring of blood pressure will be even better than the intermittent records.

1.2. Current methods for non-invasive blood pressure measurement

It is the imperfect of non-invasive blood pressure measurement techniques mainly obstructing the development of long-term and continuous blood pressure monitoring. For instance, the gold standard of non-invasive BP measurement, i.e. the auscultatory method, is unsuitable for this new type monitoring because it has to use a bulky cuff, should be operated by a trained physician and can only provide intermittent values of BP. Other measurement methods, such as the oscillometric, tonometric or volume-clamp methods, also suffer from one or more of these drawbacks.

1.2.1. The auscultatory method (mercury sphygmomanometer)

The auscultatory method, which has become the most common method and gold standard of non-invasive blood pressure measurement, usually uses a cuff, a mercury manometer and a stethoscope (Fig. 1.3). The cuff with an appropriate size is placed around the upper arm at the same vertical height as the heart and connected to a mercury manometer. When the cuff is air inflated by a small hand bulb, the mercury manometer can measure the absolute pressure inside the cuff by reading the height of a column of mercury. The stethoscope is located at the elbow to amplify the pulsatile sounds from the brachial artery. At the beginning of the measurement, an operator inflates the cuff to totally occluding the brachial artery of the subject and then slowly releases the internal cuff pressure until no pulsatile sound can be heard. Because of the turbulent blood flow and oscillations of the arterial wall, the first clear tapping sound of heart pumping (the first phase of the Korotkoff sounds) will appear when the cuff pressure is equal to the systolic pressure. And the pulsatile sounds will be gradually disappeared (the fifth phase of the Korotkoff sounds) when the cuff pressure decreases to the diastolic pressure.

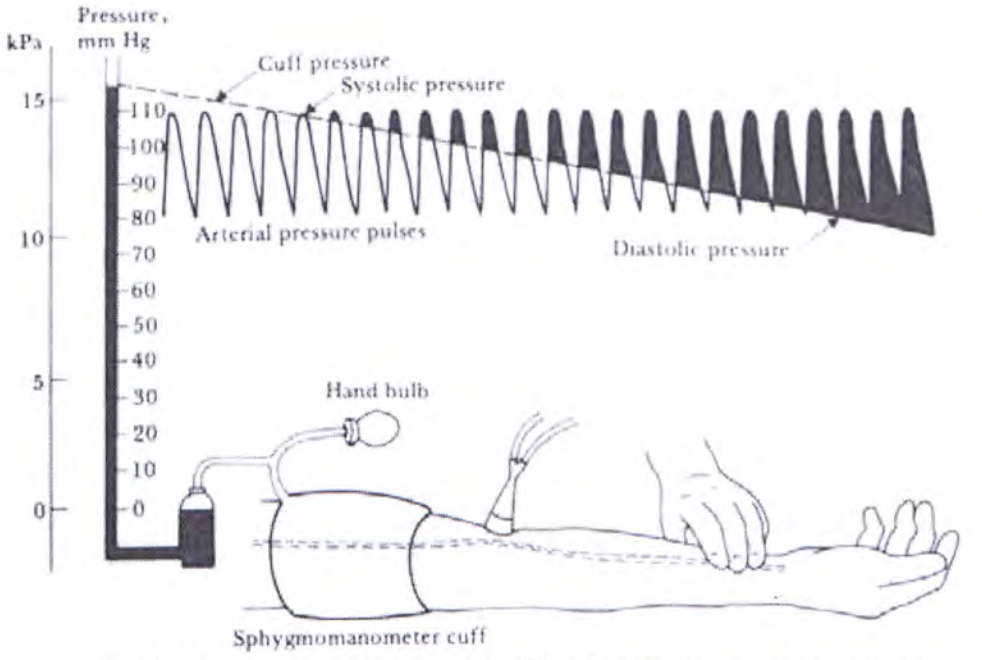

Fig. 1.3 The auscultatory method of blood pressure measurement [12]

Since the recognition of Korotkoff sounds is the key point of this method, the auscultatory measurement should be operated by trained observers. There is the possibility for measurement error due to differences in hearing acuity from observer to observer. In older patients with a wide pulse pressure, the Korotkoff sounds may become inaudible between systolic and diastolic pressure. In pregnant women, patients with arteriovenous fistulas, and aortic insufficiency, the sounds are audible even after complete deflation of the cuff [13]. Thus, it is mostly applied for routine clinic use and not recommended for home healthcare.

1.2.2. The oscillometric method

The oscillometric method uses cuff occlusion and external pressure as the same as the auscultatory method. During the graduate cuff deflation, the point of maximal oscillation corresponds to the mean intra-arterial pressure (Fig. 1.4). The systolic and diastolic pressures are estimated indirectly according to some experienced equations. Since no transducer need be placed over the brachial artery in the oscillometric, the placement of the oscillometric cuff is not as critical as the auscultatory method. And

this method has been successfully automated for self-use at home.

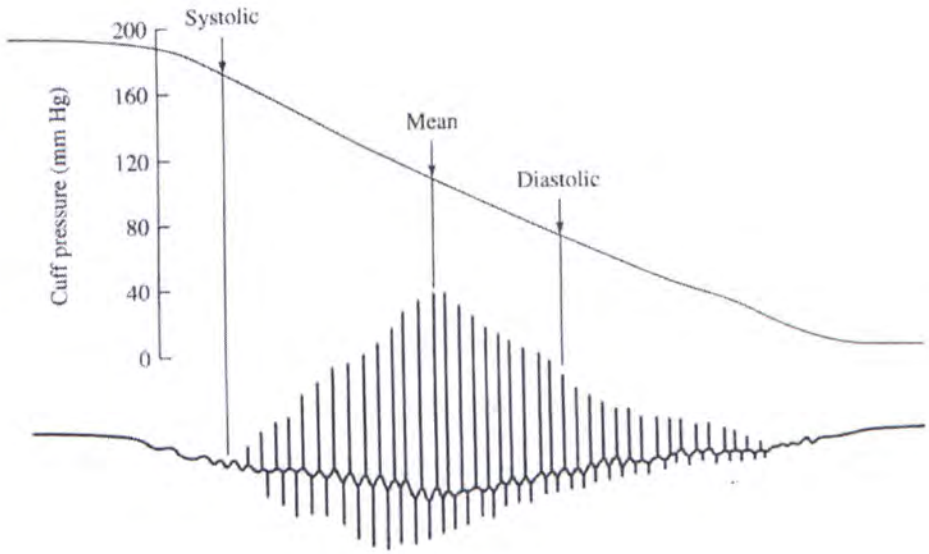

Fig. 1.4 The oscillometric method [12]

However, the main problem with this technique is the oscillation amplitude depends on several factors of which blood pressure is only one. The stiffness of the arteries influences the oscillation largely. Thus, people with stiff arteries and wide pulse pressures the mean arterial pressure may be significantly underestimated [14]. On the other hand, dramatic differences of estimated systolic blood pressure between devices has been shown, which is caused by using different proprietary algorithms [15]. From the aspect of long term monitoring, though it has been used for recording intermittent blood pressure in the 24-hour ambulatory monitoring, this method dose not work well during physical activities since motion artifact is a considerable noise source.

Besides, the biggest drawback of the oscillometric method, as well as the auscultatory method, is the bulkiness and discomfort of the inflatable cuff. The air pump limits the minimization of equipment while the repeating occlusion of arteries disturbs the normal routine of users, especially in mobile or sleeping environment. It can be predict that methods with inflatable cuffs are not promising ways for long term and continuous blood pressure monitoring.

1.2.3. The tonometric method

The tonometry method of arterial BP measurement is first developed by Pressman and Newgard in 1961 [16]. The principle of this technique is that when an artery is partially compressed or splinted against a bone, the pulsations are proportional to the internal pressure [13]. The pulsation signal of arteries is usually detected at the wrist by a pressure transducer or transducer array which needs to be positioned directly contacting the skin with a suitable pressure. The absolute signal values are mainly depended on the angle and location of sensors so that tonometry only provides the pressure waveform. Individual calibration, such as the cuff techniques mentioned above, is necessary for each time of sensor replacement in order to gain the estimated pressures [17].

Compared to auscultatory and oscillometric methods, the tonometry has innovated a new way to get continuous blood pressure continuously non-invasively other than intermittent values. However, too sensitive to motion artifact and lack of efficient calibration methods have bounded its further application. Studies of Smulyan et al. have shown that, even in the quiet and resting state, there are still large scatters between the estimated aortic pressure by tonometry and the true values recorded from aortic catheterization [18]. Moreover, the cost of the tonometric pressure sensors is still expensive until now. Thus, this technique is far from commercialization for a wide application.

1.2.4. The volume-clamp method

In the volume-clamp method, the arterial pulsation in a finger is detected by a photoplethysmography under an inflatable cuff. The output of the photoplethysmography is feeding back rapidly to adjust the cuff pressure in order to keep no pulsation on the arterial wall, i.e. "unloaded arterial wall" [19]. In this "balanced" situation, the transmural pressure of the arterial wall is supposed to be

zero so that the external pressure can represent the internal arterial pressure. Thus, this method can assess the arterial blood pressure and its short-term changes by tracking the accurate pressure of the finger cuff. It is a great innovation in the area of continuous and non-invasive blood pressure monitoring.

However, the pressure wave tracked by finger cuff may be different from central intra-arterial pressure wave both in shape and magnitude [20]. This unloading technique cannot discriminate pressure changes caused by variation of peripheral vascular tone [21]. In addition, a constant and continuous external pressure on the skin surface will cause hemodynamic and reflex vascular changes [22] so that the volume-clamp method only gives estimation of pressure variation but will under- or over-estimate the central blood pressure when compared with the traditional measurement results. That is to say, it is relative inaccurate for measuring absolute levels of blood pressure [13].

On the other hand, sensitive pressure sensors and a rapid feedback system are required in use of this method while inflatable cuffs are still necessary for measurement and calibration. Due to these requirements, the equipments of volume-clamp method are high in price and bulky in size, which has restricted its clinical application.

1.3. Blood pressure estimation based on pulse arrival time

According to the introduction in Section 1.2, it is the current situation that none of the existing technologies are fully satisfied the demand of a long term and continuous BP monitoring. An ideal technique for this purpose should satisfy that: 1) it can monitor blood pressure non-invasively and continuously; 2) no inflatable cuff is included and the equipment is small, light and comfortable; 3) the cost is low as well as the method is simple to be operated, especially for home healthcare.

The method of blood pressure estimation based on pulse arrival time (PAT) has been shown its great potential to fulfill all these requirements above. PAT, the main parameter used in PAT-BP estimation, describes the time that pressure pulses transits from their generation by left ventricular to their arrival to a peripheral site. According to the hemodynamic theories, the propagation properties of pressure pulsation are largely decided by the inter-arterial pressure. There is a high correlation between BP and PAT, and the PAT is sensitive to beat-to-beat BP variations [23]-[26]. Meanwhile, because pulses in different locations of cardiovascular system can be continuously detected by external transducers such as electrocardiogram (ECG) electrodes and photoplethysmogram (PPG) sensors, the blood pressure can be estimated beat by beat without cuffs. Moreover, both kinds of these transducers are small, light and easily implemented so that the size and weight of devices can be minimized. Therefore, the idea is attractive to develop a small-size, continuous and cuffless BP monitoring device based on PAT measurement.

However, the quasi-linear relationship between BP and PAT largely depends on the individual and external conditions so that how to calibrate the estimation equation for a specific subject becomes a main challenge.

Up to now, the cuff-based individual calibration [27][28] is the most widely accepted calibration method for PAT-BP estimation but using BP readings from auscultatory or oscillometric method conflicts the objective of cuffless measurement. Cuffless calibration methods, for example the calibration based on hydrostatic pressure [29] and the machine learning calibration by a group of subjects [30], suffer from one or more drawbacks such as too complicated operation conditions, lacking of theoretical explanation, and low estimation accuracy. In a word, though different kinds of methods have been proposed for improving efficiency and accuracy, the investigation of cuffless approaches of PAT-BP calibration and estimation is far from ending yet.

1.4. Objectives and structures of this thesis

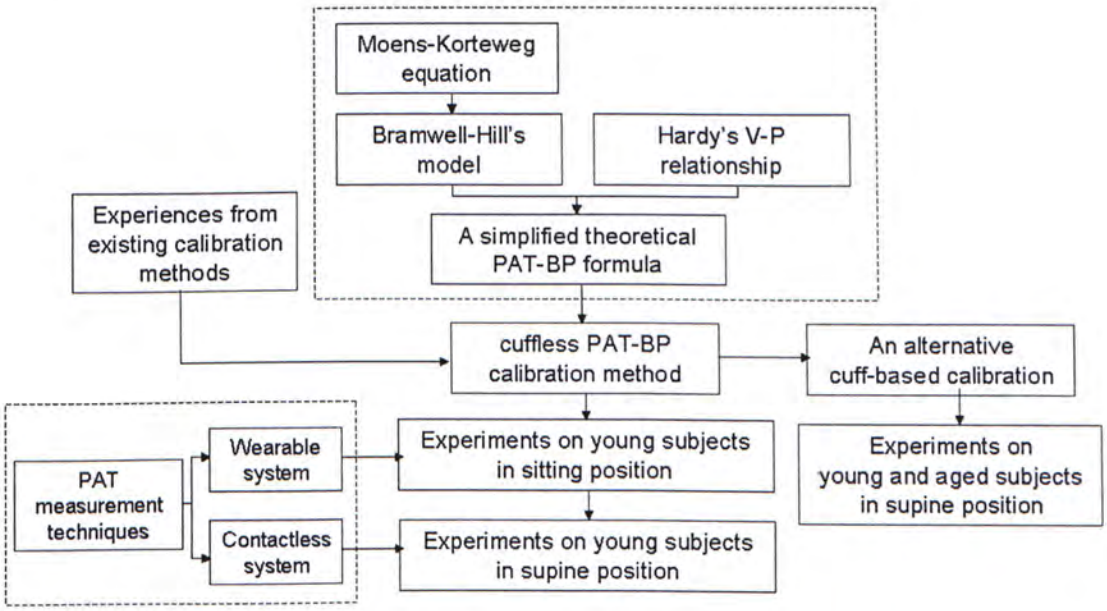

Fig. 1.5 Structures of the whole study in this thesis

The purpose of this thesis is to investigate the cuffless calibration and estimation methods for continuous arterial blood pressure monitoring based on pulse arrival time. Fig. 1.5 gives an overview of structures of the whole study in this thesis. This thesis is mainly divided into six chapters:

Chapter 1 gives a brief introduction of the importance of long term and continuous blood pressure monitoring and reviews the current development status of non-invasive blood pressure measurement methods.

The hemodynamic principle of pressure pulse propagating along arterial walls is explained in Chapter 2, which is the theoretical foundation of PAT-BP estimation. A simplified PAT-BP formula will be given upon a detailed deduction from the Moens-Korteweg equation, Bramwell-Hill's model and Hardy's volume-pressure (V-P) relationship.

Chapter 3 discusses how to implement the PAT-BP estimation for practical application, and mainly focuses on the comparison of several calibration methods for

the estimation. A new cuffless calibration approach will be proposed based on both the theoretical formula and the practical experiences from the existing methods.

Chapter 4 tests the proposed calibration method on a young and healthy group of 35 subjects. This new method is successful during the experiments conducted in sitting position but is not so efficient in supine position. In addition, both wearable and contactless systems designed for PAT measurement are introduced and evaluated by experiments in Chapter 4.

Further investigation of this problem is given in Chapter 5 with experiments applied on 20 young subjects and 20 aged subjects. An alternative cuff-based calibration is offered for supine position in Chapter 5.

Finally, conclusion of this thesis has been given in Chapter 6.

Reference

[1]. A Dictionary of Public Health. Ed. John M. Last, Oxford University Press, 2007. Oxford Reference Online.

[2]. Textbook of Medical Physiology, 7th Ed., Guyton & Hall, Elsevier-Saunders, pp. 220.

[3]. Concise Medical Dictionary. Oxford University Press, 2007. Oxford Reference Online.

[4]. T.G. Pickering, N.H. Miller, G. Ogedegbe, L.R. Krakoff, N.T. Artinian, D. Goff, "Call to Action on Use and Reimbursement for Home Blood Pressure Monitoring: Executive Summary A Joint Scientific Statement From the American Heart Association, American Society of Hypertension, and Preventive Cardiovascular Nurses Association," Hypertension, 2008 (52) pp.1-9.

[5]. E. Dolan, A. Stanton, L. Thijs, K. Hinedi, N. Atkins, S. McClory, E. D. Hond, P. McCormack, J. A. Staessen, E. O'Brien, "Superiority of Ambulatory Over Clinic Blood Pressure Measurement in Predicting Mortality The Dublin Outcome Study," Hypertension, 2005 (46) pp.156-161.

[6]. D. Clement, M. De Buyzere, D. De Bacquer, P. De Leeuw, D. Duprez, R. Fagard, P. Gheeraert, L. Missault, J. Braun, R. Six, P. Van Der Niepen, E. O'Brien, "Prognostic value of ambulatory blood-pressure recordings in patients with treated hypertension," New England Journal of Medicine, 2005(10) pp. 2407-2415.

[7]. Y. Shintani, M. Kikuya, A. Hara, T. Ohkubo, H. Metoki, K. Asayama, R. Inoue, T. Obara, Y. Aono,

T. Hashimoto, J. Hashimoto, K. Totsune, H. Hoshi, H. Satoh and Y. Imai, "Ambulatory blood pressure, blood pressure variability and the prevalence of carotid artery alteration: the Ohasama study," J. Hypertension, 2007 (25) pp. 1704-1710.

[8]. R. Marfella, M. Siniscalchi, M. Portoghese, C.D. Filippo, F. Ferraraccio, C. Schiattarella, B. Crescenzi, P. Sangiuolo, G. Ferraro, S. Siciliano, F. Cinone, G. Mazzarella, S. Martis, M. Verza, L. Coppola, F. Rossi, M. D'Amico, G. Paolisso, "Morning Blood Pressure Surge as a Destabilizing Factor of Atherosclerotic Plaque Role of Ubiquitin–Proteasome Activity," Hypertension, 2007 (49) pp.784-791.

[9]. K. Kario, T.G. Pickering, Y. Umeda, S. Hoshide, Y. Hoshide, M. Morinari, M. Murata, T. Kuroda, J.E. Schwartz, K. Shimada. "Morning surge in blood pressure as a predictor of silent and clinical cerebrovascular disease in elderly hypertensives: a prospective study," Circulation, 2003 (107) pp.1401–1406.

[10]. P. Gosse, R. Lasserre, C. Minifie, P. Lemetayer, J. Clementy. "Blood pressure surge on rising," J. Hypertension, 2004 (22) pp.1113–1118.

[11]. H. Metoki, T. Ohkubo, M. Kikuya, K. Asayama, T. Obara, J. Hashimoto, K. Totsune, H. Hoshi, H. Satoh, Y. Imai, "Prognostic significance for stroke of a morning pressor surge and a nocturnal blood pressure decline: the Ohasama study," Hypertension, 2006 (47) pp.149 –154.

[12]. John G. Webster, "Medical Instrumentation: Application and Design," 3rd Ed., 1998.

[13]. T. G. Pickering, J. E. Hall, L. J. Appel, B. E. Falkner, J. Graves, M. N. Hill, D. W. Jones, T. Kurtz, S. G. Sheps, E. J. Roccella, "Recommendations for blood pressure measurement in humans and experimental animals: part 1: blood pressure measurement in humans: a statement for professionals from the subcommittee of professional and public education of the American heart association council on high blood pressure research," circulation, 2005(111) pp.697-716.

[14]. V. Montfrans, "Oscillometric blood pressure measurement: progress and problems," Blood Pressure Monitoring. 2001(6) pp.287–290.

[15]. J.N. Amoore, D.H. Scott, "Can simulators evaluate systematic differences between oscillometric non-invasive blood-pressure monitors," Blood Pressure Monitoring, 2000(5) pp.81– 89.

[16]. G. L. Pressman, and P. M. Newgard, "A Transducer for the Continuous External Measurement of Arterial Blood Pressure," IEEE Transactions on Bio-medical Electronics, 1961(10) pp.73-81.

[17]. K. Matthys and P. Verdonck, "Development and modelling of arterial applanation tonometry: A review," Technology and Health Care, 2002(10) pp.65-76.

[18]. H. Smulyan, D. S. Siddiqui, R. J. Carlson, G. M. London, M. E. Safar, "Clinical Utility of Aortic Pulses and Pressures Calculated From Applanated Radial-Artery Pulses," hypertension, 2003(42) pp.150-155.

[19]. J. Pefiaz, "Photoelectric measurement of blood pressure, volume and flow in the finger," Digest of the Int. Conf. on Medicine and Biological Engineering, Dresden, 1973, pp.104.

[20]. L. W. J. Bogert and J. J. V. Lieshout, "Non-invasive pulsatile arterial pressure and stroke volume changes from the human finger," Exp. Physiol, 2005(90) pp.437-446.

[21]. W. J. Kaspari and R. A. Stem, "Apparatus and method for noninvasive blood pressure measurement," US Patent, No. 5533511, 1996.

[22]. R. P. Schnall, N. Gavriely, S. Lewkowicz, and Y. Palti, "A rapid noninvasive blood pressure measurement method for discrete value and full waveform determination," J. Appl. Physiol., 1996(80) pp. 307-314.

[23]. L Geddes and M Voelz, "Pulse Transit Time as an Indicator of Arterial Blood Pressure," Psychophysiology, 1981(18) pp. 71-74.

[24]. K. Chan and Y. Zhang, "Noninvasive and cuffless measurement of blood pressure for telemedicine," 2001 Proceeding of the 23 rd Annual EMBS International Conference, Istanbul, Turkey, 2001, pp. 3592-3593.

[25]. W. Chen, T. Kobayashi, S. Ichikawa, Y. Takeuchi, T. Togawa, "Continuous estimation of systolic blood pressure using the pulse arrival time and intermittent calibration," Medical & Biological Engineering & Computing, 2000(38) pp. 569-574.

[26]. Y. Yoon, J. Cho, G. Yoon, "Non-constrained Blood Pressure Monitoring Using ECG and PPG for Personal Healthcare," Journal of Medicine System, 2009(33) pp. 261–266.

[27]. C. Poon and Y. Zhang, "Cuff-less and noninvasive measurements of arterial blood pressure by pulse transit time", 27th Annual International IEEE EMBS Conference, Shanghai, China, 2005, pp.5877-5880.

[28]. Y. Yan and Y. Zhang, "A Novel Calibration Method for Noninvasive Blood Pressure Measurement Using Pulse Transit Time", Proceedings of the 4th IEEE-EMBS International Summer School and Symposium on Medical Devices and Biosensors, St Catharine's College, Cambridge, UK, 2007, pp.22-24.

[29]. D. McCombie, A Reisner, and H Asada, "Motion Based Adaptive Calibration of Pulse Transit Time Measurements to Arterial Blood Pressure for an Autonomous, Wearable Blood Pressure Monitor", 30th Annual International IEEE EMBS Conference, Vancouver, British Columbia, Canada, 2008, pp.989-992.

[30]. S. Suzuki and K. Oguri, "Cuffless Blood Pressure Estimation by Error-Correcting Output Coding Method Based on an Aggregation of AdaBoost with a Photoplethysmograph Sensor", 31st Annual International IEEE EMBS Conference, Minneapolis, USA, 2009, pp.6765-6768.

2. Hemodynamic models: relationship between PAT and BP

2.1. The generation of arterial pulsation

In each heart period, the left ventricular contracts and the aorta valves open so that the blood flow is pushed into aorta making the elastic aortic wall expand (Fig. 2.1). Then the left ventricular widens, the aorta valves close, and the blood flow travels forward by the passive contraction of aorta (Fig. 2.2). After passing the capillaries, the veins, and the pulmonary circulation, blood returns to the left ventricular starting a new systemic circulation. These procedures repeat time and time again so that the expansion and contraction of aorta are periodically continued.

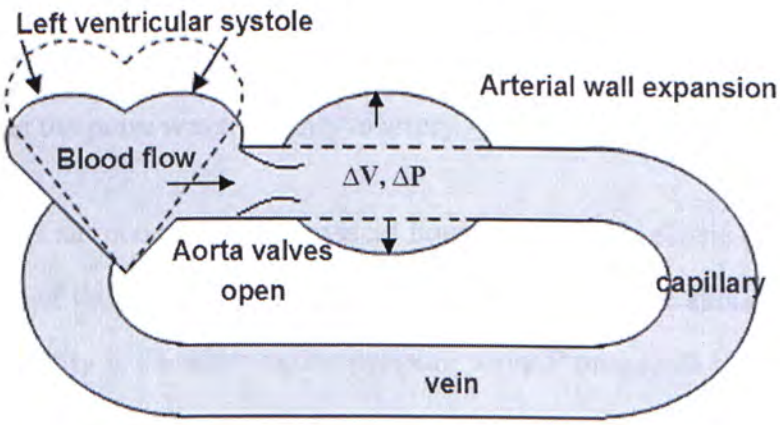

Fig. 2.1 Left ventricular systole

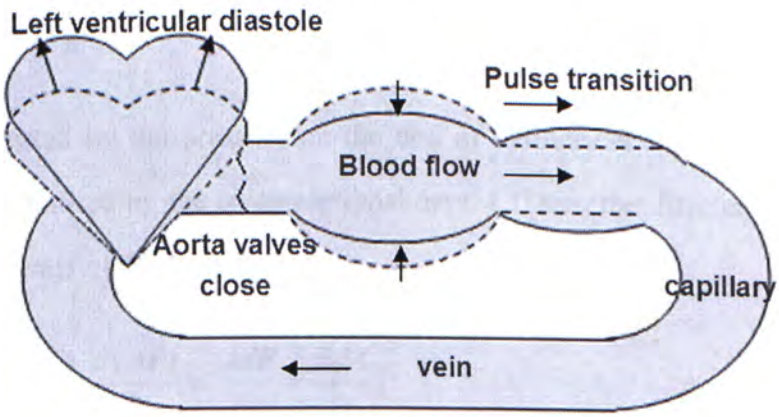

Fig. 2.2 Left ventricular diastole

Corresponded to the movement of aorta, fluctuation along arterial walls has been generated. This fluctuation is one kind of solid material vibrations, transiting as a pressure wave with power. Though the original power generating the pressure pulses is the flowing of the blood, the propagation principles of pressure and flow waves in arterial vessels are totally different from each other. It should be noted that, the propagation velocity of arterial wall is much faster than it of blood flow. Several hemodynamic models have been built up to describe the propagation of arterial pressure waves.

2.2. Pulse wave velocity along the arterial wall

2.2.1. Moens-Korteweg equation [1][2]

In 1878, Moens and Korteweg derived a mathematical expression to calculate the pressure wave velocity traveling along an elastic tube. It is the most popular model for explaining the pulse wave velocity in artery.

Supposing it is an incompressible inviscid liquid flows in an elastic cylindrical tube, every particle of this liquid in the tube is moving parallel to the axis of the tube with a constant velocity v. Considering the pressure wave P propagate a distance of dx in a time of dt, the pulse velocity c of the pressure wave can be expressed as:

$$c = \frac{dx}{dt}. \qquad \text{Eq. 2.1}$$

The force exerted by the pressure on the end of cylindrical liquid length dx is the pressure P multiplied by the cross-sectional area A. Thus, the difference of the force between both ends of the liquid is

$$\frac{dF}{dx} = \frac{d(AP)}{dx} = \frac{AdP}{dx} + \frac{PdA}{dx}. \qquad \text{Eq. 2.2}$$

Supposing the displacement of the internal radius of the tube R is small, the $\frac{PdA}{dx}$ is negligible, i.e.

$$\frac{dF}{dx} \approx \frac{AdP}{dx} = \frac{\pi R^2 dP}{dx}. \qquad \text{Eq. 2.3}$$

Considering the density of liquid ρ, the mass of the liquid should be $\rho\pi R^2 dx$. In addition, because the axial acceleration of the liquid is $\frac{dv}{dt}$, according to Newton's second low $F=ma$, there is

$$\pi R^2 dP = \rho\pi R^2 dx \cdot \frac{dv}{dt} \qquad \text{Eq. 2.4}$$

i.e.,

$$\frac{dP}{dx} = \rho\frac{dv}{dt}. \qquad \text{Eq. 2.5}$$

From the aspect of inflow and outflow of liquid volume, the changes of the volume flow Q in the segment of dx can be expressed as

$$\frac{dQ}{dx} = \frac{dV/dt}{dx} = \frac{2\pi RdRdx/dt}{dx} = \frac{2\pi RdR}{dt}, \qquad \text{Eq. 2.6}$$

Alternatively, dQ is equal to the flow velocity multiplied the cross-sectional area so that

$$\frac{dQ}{dx} = \frac{d(vA)}{dx} \approx \frac{\pi R^2 dv}{dx}. \qquad \text{Eq. 2.7}$$

Combining Eq. 2.6 and Eq. 2.7 together, we can get

$$\frac{dR}{dt} = \frac{Rdv}{2dx}. \qquad \text{Eq. 2.8}$$

On the other hand, the force per unit area that produces the deformation is called the stress; the deformation described as the ration of the deformation to its original form. According to Hooke's low, within certain limits, strain is proportional to stress. The relationship between stress and strain is expressed as an elastic modulus. Supposing the elastic modulus of the tube wall is E and the thickness of the wall is h, there is

$$E = \frac{stress}{strain} = \frac{RdP}{h} \cdot \frac{R}{dR}, \qquad \text{Eq. 2.9}$$

so that

$$dR = \frac{dP}{h} \cdot \frac{R^2}{E}. \qquad \text{Eq. 2.10}$$

Combining Eq. 2.8 and Eq. 2.10 together, there is

$$\frac{dP}{dt} = \frac{Eh}{2R} \cdot \frac{dv}{dx}. \qquad \text{Eq. 2.11}$$

Differentiating Eq. 2.5 by x and differentiating Eq. 2.11 by t, there are

$$\frac{d^2P}{dx^2} = \rho \frac{d^2v}{dxdt} \qquad \text{Eq. 2.12}$$

and

$$\frac{d^2P}{dt^2} = \frac{Eh}{2R} \frac{d^2v}{dxdt}. \qquad \text{Eq. 2.13}$$

Thus, pulse wave velocity can be described as:

$$(\frac{dx}{dt})^2 = c^2 = \frac{Eh}{2\rho R} \qquad \text{Eq. 2.14}$$

i.e. the Moens-Kerteweg equation:

$$c = \sqrt{\frac{Eh}{2\rho R}}, \qquad \text{Eq. 2.15}$$

where c is the wave velocity, E is Young's modulus, h is the thickness of tube wall, ρ is the density of blood and R is the radius of tube wall. Obviously, the elastic and geometric properties of the arterial wall play important roles in determining propagation of pressure waves. In the coming sections, the connections between elastic properties of arteries and blood pressure will be built up so that the propagation time and pressure are finally linked together.

2.2.2. Bergel wave velocity [1][3]

The assumptions underlying the Moens-Korteweg equation are that the tube has a thin wall (i.e. *h/2R* is small) and is filled with an ideal incompressible inviscid liquid. The value of *h/2R* is normally less than 0.1and the bulk modulus of water is between 10^3 and 10^4 times greater than the elastic modulus of the wall. In large arteries, the effect of viscosity is also small, but it will greatly retard the velocity in the smaller arteries.

The errors due to assuming that the wall is thin have been explored by Bergel in 1960. In a wall of finite thickness, the Poisson's ratio σ must be considered. Poisson's ratio is the ratio, when a sample object is stretched, of the contraction or transverse strain to the extension or axial strain. The Poisson's ratio of a stable, isotropic, linear elastic material cannot be less than −1.0 nor greater than 0.5 due to the requirement that the elastic modulus, the shear modulus and bulk modulus have positive values.

Most materials have Poisson's ratio values ranging between 0.0 and 0.5 [4]. The full correction equation by Bergel is given as

$$\left(\frac{c_t}{c}\right)=\frac{(2-\gamma)}{[2-2\gamma(1-\sigma-2\sigma^2)+\gamma^2(1-\sigma-2\sigma^2)-2\sigma^2]}, \qquad \text{Eq. 2.16}$$

where c_t is the 'true' derived velocity, r is the ratio h/R_{outer}. Taking a Poisson ratio of 0.5, the true derived velocity c_t is 15% higher than calculated velocity c from Eq. 2.15 even if the wall is thin. An effective simplification of Eq. 2.16 in terms of Eq. 2.15 is

$$c_t=\sqrt{\frac{Eh}{2\rho R(1-\sigma^2)}}. \qquad \text{Eq. 2.17}$$

Compared Eq. 2.17 with Eq. 2.15, only a new parameter, Poisson ratio, is introduced into the equation. It is a subject-dependent parameter of material properties, which will not be changed with variables we concerned in blood pressure estimation, such as pressure, velocity and transit distance. Thus, σ can be treated as a constant and the difference between Moens-Korteweg and Bergel equations can be ignored when subject calibration is applied. The Moens-Korteweg equation will be the main one in the following discussion

2.3. Relationship between PWV and BP

Researchers have found that the elasticity of arterial wall is pressure-dependent. Hardy and Collins collected the experiment results to create a hypothesis describing how the volume of arteries will be changed with the blood pressure. Hughes conducted several in-vivo and in-vitro experiments to get an exponential equation between blood pressure and Young's modulus directly. Upon these empirical formulas and the hemodynamic deduction above, the relationship between PWV and blood pressure is established.

2.3.1. Bramwell-Hill's model [5]

According to Bramwell-Hill's derivation, a small rise dP in pressure may shown to cause a small increase in radius as in Eq. 2.10, or a small increase in volume V per length dx, i.e.

$$V = \pi R^2 dx \qquad \text{Eq. 2.18}$$

$$dV = 2\pi R dR \cdot dx = \frac{2\pi R^3 dx dP}{Eh} \qquad \text{Eq. 2.19}$$

$$\frac{V}{dV} = \frac{Eh}{2R \cdot dP} \qquad \text{Eq. 2.20}$$

Thus, the Eq. 2.15 and Eq. 2.16 can be respectively expressed in terms of Eq. 2.20 as

$$c = \sqrt{\frac{VdP}{\rho dV}}. \qquad \text{Eq. 2.21}$$

The equation Eq. 2.21 suggests that PWV is decided by the volume of the artery and the changes of volume with the variation of blood pressure. If the relationship between arterial volume and pressure can be verified, the PWV-BP relationship can be uncovered.

2.3.2. Volume-pressure relationship [6]

Hardy and Collins established an empirical exponential equation to describe the dependence of blood volume on the blood pressure for circulatory elements. Basing on the physiological limits that increasing pressure within a vessel leads to increasing vessel stiffness, the $\frac{dV}{dP}$ tends to zero as P increases. One preferable mathematical representation of this condition can be:

$$k(V_m - V) = \frac{dV}{dP}, \qquad \text{Eq. 2.22}$$

where k is a constant, have dimensions of compliance, characterizing the elastic property of the vessel wall and surrounding tissue while V_m is a limiting value of the vessel volume. According to this differential equation, a simplified pressure-volume formula can be obtained by integration as

$$P = P_0 - \frac{1}{k}\ln\frac{V_m - V}{V_m - V_0}, \qquad \text{Eq. 2.23}$$

where P_0 and V_0 are a pair of pressure-volume values at an arbitrary point. This equation can be rearranged into the following form:

$$V = V_m(1 - K_0 e^{-kP}) \qquad \text{Eq. 2.24}$$

where

$$K_0 = \frac{V_m - V_0}{V_m} e^{-kP_0}. \qquad \text{Eq. 2.25}$$

Substituting Eq. 2.22 and Eq. 2.25 into Eq. 2.21, there is

$$c^2 = \frac{V}{\rho} \cdot \frac{1}{k(V_m - V)} = \frac{1}{\rho k}\left(\frac{1}{K_0} e^{kP} - 1\right) \qquad \text{Eq. 2.26}$$

and

$$P = \frac{1}{k}\ln[K_0(c^2 \rho k + 1)]. \qquad \text{Eq. 2.27}$$

In order to obtain a simplified form, Eq. 2.27 is approximated as

$$P \approx \frac{1}{k}\ln(K_0 \rho k \cdot c^2), \qquad \text{Eq. 2.28}$$

where P is the blood pressure, c is the wave velocity, ρ is the density of blood, k and K_0 are the main parameters of vessel properties determining how fast c will be changed with P.

2.3.3. Hughes' model [1][7]

In 1979, Hughes et al showed that the modulus of elasticity E of the aorta increases exponentially with increasing intravascular pressure P. According to in-vitro and in-vivo experimental results, an empirical formula was achieved, i.e.

$$E = E_0 e^{\alpha P}, \qquad \text{Eq. 2.29}$$

where E_0 is the zero-pressure modulus and α is a constant, both of which depend on the site of measurement and upon the particular animal.

Substituting Eq.. 2.29 into Eq.. 2.15, there is

$$c = \sqrt{\frac{E_0 h \cdot e^{\alpha P}}{2R\rho}}, \qquad \text{Eq. 2.30}$$

i.e.

$$P = \frac{1}{\alpha}\ln\left(\frac{2R\rho}{E_0 h} \cdot c^2\right). \qquad \text{Eq. 2.31}$$

It is clear that pulse wave velocity c increases exponentially with the increase of arterial pressure P and E_0, R and h are the parameters determine how fast it will be.

In spite of the difference between specific values of coefficients in Eq. 2.28 and Eq.

2.31, both Bramwell-Hill and Hughes' equations have described a logarithmic relationship between PWV and BP. Since only two extra parameters are introduced in Bramwell-Hill equation while three in Hughes' equation, the Bramwell-Hill model is preferred to be used in this thesis.

2.4. The theoretical expression of PAT-BP relationship

The time from ventricular contraction to pulses' arrival at a peripheral site is called pulse arrival time (PAT), which consists of two parts: the left ventricular pre-ejection period (PEP) and pulse transit time (PTT). PEP is the time interval from ventricular contraction until aorta valves opening with blood ejection. PTT is the time a pressure pulse propagating from aortic wall to a specific peripheral artery. Supposing the length of pressure wave propagation along the artery is L, the PWV can be expressed by PAT as

$$PWV = c = \frac{L}{PTT} = \frac{L}{PAT - PEP}. \qquad \text{Eq. 2.32}$$

Substituting Eq. 2.32 into Eq. 2.28, the relationship between pulse arrival time and blood pressure is

$$\begin{aligned} BP &= \frac{1}{k}\ln[(\frac{L}{PAT - PEP})^2 K_0 \rho k] \\ &\approx -\frac{2}{k}\ln(PAT) + \frac{1}{k}\ln(L^2 \rho k K_0) \end{aligned}, \qquad \text{Eq. 2.33}$$

where BP is the blood pressure, PAT is the pulse arrival time, L is the pulse transit distance, ρ is the density of blood, k is a constant with dimensions of compliance and K_0 is a constant derived from boundary condition. The effect of PEP is neglected by supposing it is an individual constant.

The main assumptions underlying Eq. 2.33 are : 1) the artery is an elastic cylindrical tube with thin wall filled with incompressible inviscid fluid; 2) the externally applied

pressure to arteries and the hydrostatic pressure are negligible; 3) and the blood pressure is positive[8]. The assumption 1 and 3 are quite reasonable and assumption 2 can be controlled by proper design of measurement protocol. Several other approximations are also applied during equation deduction. According to the experiment results in this thesis and other literatures, negative effects caused by these approximations are not obvious in general.

Reference

[1]. W. Nichols and M. O'Rourke, "McDonald's blood flow in arteries – Theoretical, experimental and clinical principles," 5th edition, Oxford University Press Inc., 2005.

[2]. J. Lin, "Experimental study of the modeling blood vessel corrugation effects on pulsed wave velocity," Thesis for master's degree, National Cheng Kung University, Taiwan, 2008.

[3]. X. Zhang, R. Kinnick, M. Fatemi and J. Greenleaf, "Noninvasive method for estimation of complex elastic modulus of arterial vessels," IEEE trans. on Ultrasonics, ferroelectrics, and frequency control, 2005(52) pp.642-652.

[4]. H. Gercek, "Poisson's ratio values for rocks," International Journal of Rock Mechanics and Mining Sciences, 2007(44) pp. 1–13.

[5]. M. Bramwell and A. Hill, "The velocity of the pulse wave in man," Proceedings of the Royal Society of London, 1922 pp.298-306.

[6]. H. Hardy and R. Collins, "On the pressure-volume relationship in circulatory elements," Med. & Biol. Eng. & Comput., 1982(20) pp.565-570.

[7]. D. Hughes, C. Babbs, L. Geddes, and J. Bourland, "Measurement of Young's modulus of elasticity of the canine aorta with ultrasound," Ultrasonic Imaging, 1979(1) pp.356-367.

[8]. C. Poon, "A Bio-model-based Cuffless Technique for Non-invasive and Continuous Measurement of Arterial Blood Pressure." PhD thesis, The Chinese University of Hong Kong, HK, 2007.

3. Estimation and calibration of arterial BP based on PAT

Though the theoretical PAT-BP relationship can be established as the description in Chapter 2, there are more details should be considered for practical application. This chapter will discuss how to implement PAT-BP estimation by ECG and PPG signal and how to improve the estimation accuracy in practice.

3.1. PAT measurement

As mentioned in Section 1.3, the most common method of PAT calculation is based on the measurement of electrocardiogram (ECG) and photoplethysmogram (PPG):

3.1.1. Principle of ECG measurement

The ECG signal records the electrical activity of cardiac muscles. In each period of ECG signal, the largest peak, i.e. R wave, represents the muscle activity conducting ventricular contraction, which kind of activities represents the start of blood pressure pulse generation.

In traditional measurement the ECG electrodes have to contact the skin of the limbs and chest wall directly [1]. The 12-lead ECG is the typical configuration of the ECG equipment, which can give a detailed cardiac electrical activity by ten electrodes placed as the following table [2] (Table 3.1). However, for the use of PAT measurement, the main ECG characteristic we interest in is and only is the R-peak. Thus even one lead can give the sufficient information. In experiments of this thesis, only the lead I ECG, i.e. the signal between the right arm and the left arm, was acquired by self-designed contact electrodes.

In addition, for the purpose of equipment mobilization and meeting the requirement of home healthcare, wearable and contactless measurements of ECG have been developed with the invention of electronic textile, where users are not required to put on any electrodes. These innovative techniques will be tested and evaluated in experiments of this thesis.

Table 3.1 Placement of ECG electrodes [2]

ELECTRODE LABEL	ELECTRODE PLACEMENT
RA	On the right arm, avoiding bony prominences
LA	In the same location that RA was placed, but on the left arm this time.
LL	On the left leg, avoiding bony prominences.
V1	In the fourth intercostal spaceto the right of the sternum.
V2	In the fourth intercostal space to the left of the sternum.
V3	Between leads V2 and V4.
V4	In the fifth intercostal space in the midclavicular line.
V5	Horizontally even with V4, but in the anterior axillary line.
V6	Horizontally even with V4 and V5 in the midaxillary line.

3.1.2. Principle of PPG measurement

PPG measures the volumetric changes in the blood vessels of the skin so that the pulsations in peripheral arteries can be detected. The principle of this measurement is based on the non-invasive detection of the intensity of light transmitted through, or reflected back from, a vascular tissue under the skin [4]. Once a certain skin is illuminated by a light source, less light will reach the light-detection sensor when the blood volume increases and more light does when it decreases.

The pairs of LED and photodiode are usually designed as PPG sensors. For the peripheral area of the human body which is thin enough to let the light transmit though, such as the fingers, toes, or earlobe, the transmission mode of PPG measurement can be used, i.e. the LED illuminates the tissue on one side and photodiode received the transmitted light on the other side. However, for central

areas such as the wrist or back, too thick for light transmission, only the reflection mode can be applied (Fig. 3.1).

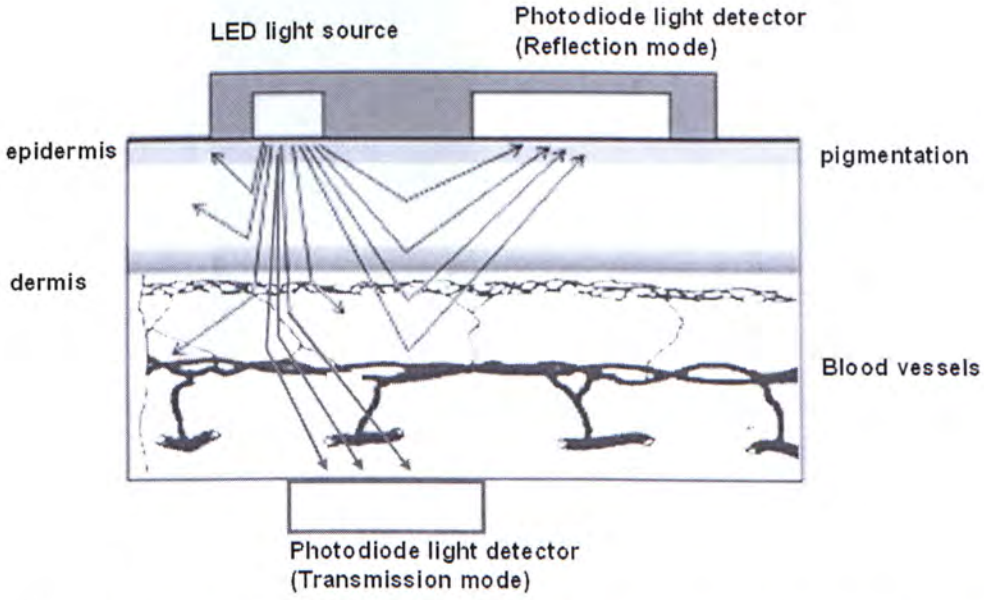

Fig. 3.1 Transmission and Reflection modes of PPG detection (graph revised from [3])

The signal detected from any site on the skin by PPG all consists of two components. As shown in Fig. 3.2 they are: a steady component (DC), which is related to the changes of blood volume in the non pulsatile component of the tissue, and a pulsatile component (AC), which is related to changing arterial blood volume [5]. Though it is relatively much smaller than the DC component, the AC component, which is mostly dependent on the pulsatile arterial blood volume, is the target signal for PAT calculation. In experiments of this thesis, the DC component of PPG will be excluded in advance while the AC part is amplified.

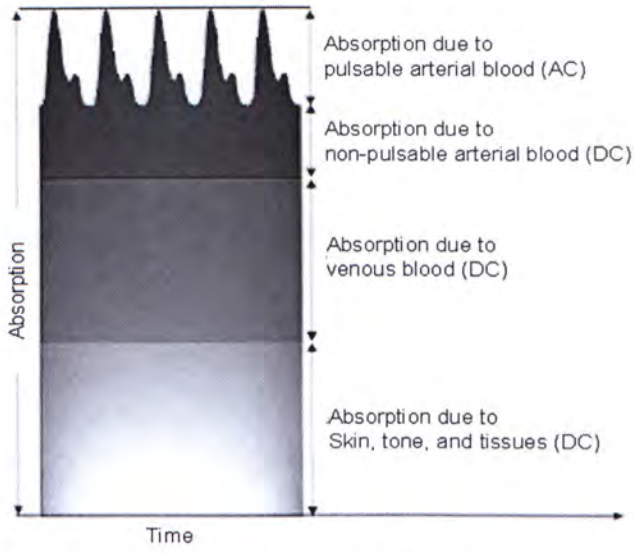

Fig. 3.2 The components of PPG signal [6]

Similar as the invention of contactless ECG measurement, contactless PPG measurement sensors have been designed in order to satisfy the requirement for wider application. Since the hardware design is not the main part of this thesis, further information about the design of wearable and contactless systems will be briefly introduced with experiment description while more attentions will be paid on testing and evaluating the efficiency of these systems.

3.1.3. Calculation of PAT

ECG and PPG signals represent the activities of both the heart and the peripheral arteries. The pulse arrival time can be decided by these two signals which are simultaneously recorded. As shown in Fig. 3.3, PAT can be defined as the time interval from ECG R-wave peak to the on-set point, also called the foot point, of the PPG wave during the same cardiac cycle. Sometimes, the peak of first derivative wave of PPG is substituted the on-set point because of the identification difficulty of on-set point.

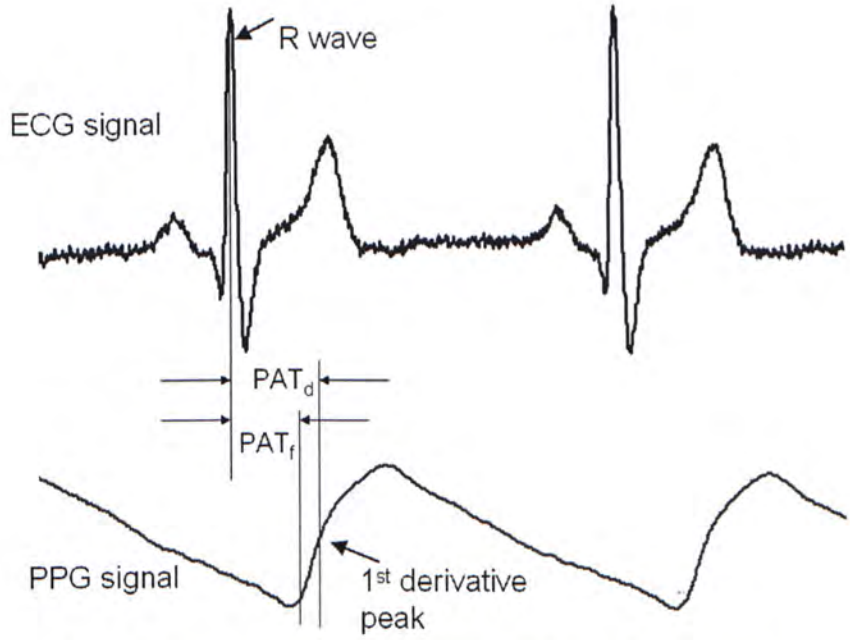

Fig. 3.3 The measurement of PAT by ECG and PPG signals

Moreover, the combination of ECG and PPG is not the only way for PAT measurement, while there are some other methods, such as by phonocardiogram, ultrasound, tonometry, and so on. However, according to the description mentioned above, the PAT measurement by ECG and PPG not only has the similar accuracy as those other methods, but also: 1) needs only simple electrical and optical sensors; 2) is much easier to be operated by any un-trained person; 3) and has a low cost for system design. Thus, it is treated as a better choice in this thesis.

3.2. Calibration methods for PAT-BP estimation

In Chapter 2, a simplified PAT-BP theoretical equation has been deduced as:

$$BP = -\frac{2}{k}\ln(PAT) + \frac{1}{k}\ln(L^2 \rho k K_0) \qquad \text{Eq. 2.33}$$

where ρ is the density of blood, L is the distance travelled by the pulse, k is a constant with dimensions of compliance and K_0 is a constant derived from boundary condition. All these four parameters should be determined in advance of making PAT-BP estimation. Nevertheless ρ could be considered as a constant equal to 1055 kg/m^3 [8]

and the distance of pulse transition can be roughly measured, the values of k and K_0 are still difficult to be evaluated directly by non-invasive method. Therefore, how to calibrate these coefficients in PAT-BP equation is the key problem for the cuffless and continuous BP estimation by PAT.

Moreover, it should be mentioned that the SBP has a much larger dynamic range than MBP and DBP such that there are more difficulties for SBP estimation. In most of existing researches, rarely SBP estimation results have been reported to fully meet the standard requirements of the Association for the Advancement of Medical Instrumentation (AAMI), i.e. the mean and standard deviation of measurement errors are within 5±8 mmHg and 85 subjects are included in the evaludation. Thus, the main blood pressure parameter preferring to be discussed in this thesis is the SBP.

3.2.1. Calibration based on cuff BP readings

Based on the physiological limitation, it is indicated by Eq. 2.22 and Eq. 2.25 that k and K_0 should be non-negative numbers. Thus, Eq. 2.33 could be further simplified as

$$BP = A \cdot \ln(PAT) + B, \qquad \text{Eq. 3.1}$$

where $A<0$, that is to say, there is a negative correlation between PAT and BP. This negative correlation has been widely reported [9]-[13]. Moreover, in the normal physiological range the PAT-BP logarithmic function is quasi-linear by neglecting the slight changes of the slope so that other linear or quasi-linear formulas can be used as approximate equations, such as $BP = A \cdot PAT + B$, $BP = \frac{A}{PAT} + B$, $BP = \frac{A}{PAT^2} + B$ and so on.

The cuff-based individual calibration considers the coefficients A and B in those simplified equations as individual-dependent variables so that each subject has fixed

A and *B*. The BP readings from auscultatory or oscillometric method are used to calculate them.

In C. Poon's study [14], they considered one of the two coefficients as a function of the other coefficient and used only one cuff BP reading for each subject to do the calibration. Their technique was tested on a total of 85 subjects, aged 57±29 yrs., including 36 males and 39 hypertensives, over an average period of 6.4 weeks. The reference SBP range was 122±21mmHg while the estimation error was 0.6±9.8 mmHg.

In M. Wong's work [15], they gained individual coefficients by least-squares regression in the first experiment and then test the repeatability of these coefficients in the subsequent experiment carried out half year later. 14 healthy subjects aged 26±4 years (from 21 to 34 years) and included six males participated in the repeatability test including physiological state changes by exercise. The estimation result was 1.4±10.2 mmHg with a SBP range of 103.0±11.3 mmHg.

Up to now, the Cuff-based individual calibration is the earliest invented and most widely accepted calibration method for PAT-BP estimation. However, the model used in this method is over-simplified. For instance, the coefficients *A* and *B* are not only subject-dependent but also time-varied with the changes of physiological conditions and external environment. Moreover, the introducing of inflatable cuffs for calibration procedure conflicts with the demand of cuffless measurement, lacking the portability and convenience of its application.

3.2.2. Calibration by hydrostatic pressure changes

In order to derive a simple procedure for estimating individualized coefficients without inflatable cuffs, a mode-based method under the effects of hydrostatic pressure due to hand elevation was proposed by two different groups [16][17]. Based

on the Bramwell-Hill's model (Eq. 2.21), when subjects are asked to elevate their hands, the transmural pressure P is equal to the internal blood pressure (P_i) at the horizontal level of the heart plus a hydrostatic pressure (P_h), i.e.

$$c = \sqrt{\frac{Vd(P_{in} + P_h)}{\rho dV}} \qquad \text{Eq. 3.2}$$

In a similar way, the hydrostatic pressure should be considered in the volume-pressure relationship. The empirical volume-pressure equation described in [16] was used and substituted into the above formula. After a few calculations, there are [17]:

$$PTT = \begin{cases} \dfrac{L\sqrt{\rho b}}{\sqrt{1+\exp(bP_i)}} & ; h = 0 \\ \dfrac{2L}{\sqrt{\rho b g h}} \ln \left| \dfrac{\sqrt{\exp[b(P_i - P_h)] + \exp(-bP_h)} - \sqrt{\exp(-bP_h)}}{\sqrt{\exp[b(P_i - P_h)]+1} - 1} \right| & ; h \neq 0 \end{cases}, \qquad \text{Eq. 3.3}$$

where ρ is the density of blood, L is the distance traveled by the pulse, b is a subject-dependent coefficient characterizing the artery properties, and the hydrostatic pressure $P_h = \rho g h$. PTT is a function of h for a pair of subject-dependent coefficients $\{L, b\}$ at a specific initial internal BP. If the short-time variation of internal BP at a stable physiological state is negligible, the coefficient b can be calibrated by hand elevation. Thus, BP can be estimated by PTT while $h=0$ [17]:

$$BP = \frac{1}{b} \ln\left(\frac{L^2 \rho b}{PTT^2} - 1\right). \qquad \text{Eq. 3.4}$$

The hydrostatic calibration is the one most approximated to the hemodynamic models. Theoretically, the method can achieve a precise calibration of PTT-BP equation without use any cuff BP readings. However, how to excluding PEP from PTT measurement is not properly solved yet till now, and PAT is actually the

substitute parameter used in real calculations. In addition, more inaccuracy will be introduced by the rough measurement of L and h. Thus, the hydrostatic approach should be conducted under well-controlled conditions.

Following the principle of hydrostatic theory, D. McCombie et al. invented a motion based adaptive calibration for PTT-BP estimation [18]. During the calibration stage, subjects were asked to move their hands following the instruction of operators, while the correspond variations of PTT, height of hands, and external pressure were monitored by two PPG sensor pairs, accelerometer and contact pressure sensor respectively. The required coefficients were calculated based on those dynamic data and the BPs were estimated when subjects' hands topped movement and brought to a rest on a table. Eight subjects participated in their experiment and the estimation error for mean blood pressure (MBP) was 1.3±7.1 mmHg while the range of MBP was 92.5±9.6 mmHg.

3.2.3. Calibration by multiple regression

In spite of model-based individual calibration, researchers have tried another way to find the possibility of fixing coefficients in group. Research studies have found that height, leg length, age and gender are associated with BP [19][20]. Therefore some researchers attempted to use these physiological parameters which might affect BP values to make up the difference among the PAT-BP estimation of different subjects. Their selection of parameters was mainly based on the statistical correlation analysis.

E. Park et al., proposed a regression model as [21]

$$SBP = 85.862 - 119.27PAT + 0.259weight + 0.439arm\_length, \qquad \text{Eq. 3.5}$$

where the units of *PAT*, *weight* and *arm length* were ms, kg and cm respectively. The constants in the equation were achieved from a multiple linear regression with a pool

of 35 subjects. Testing on another 10 unspecific subjects who were not included in the regression pool, they got the estimation errors within 5.8±4.2 mmHg. J. Kim et al. have done a similar research to adjust PAT-BP estimation by weight and arm length except using an algorithm of artificial neural network instead of the multiple linear regressions [22].

The main drawback of group calibration with regression is the lack of the support of theoretical model. The explanation how general physiological parameters, for example the weight, influent pulse wave propagation is weak so that the accuracy of estimation might be gained by chance.

3.3. Model-based calibration with PPG waveform parameters

According to the review in Section 3.2, it indicates that as a more efficient calibration: 1) the method should be supported by theoretical evidence; 2) its procedures should be easily operated and controlled; 3) the inflatable cuffs had better not be included. Thus, based on the theoretical models in Chapter 2 and the practical experience in Chapter 3, a new model-based calibration method using parameters from PPG waveform has been proposed in this thesis.

3.3.1. Model-based equation with parameters from PPG waveform

Eq. 2.33 can be rewritten as

$$BP = -\frac{2}{k}\ln(PAT) + \frac{2}{k}\ln(L) + \frac{1}{k}\ln(K_0) + \frac{1}{k}\ln(\rho k). \qquad \text{Eq. 3.6}$$

If the PPG sensor detects peripheral pulses from finger or wrist, then the pulse transit distance will be correlated with the arm length (This may be a reasonable explanation of the results of Section 3.2.3 why arm length can improve the PAT-BP estimation).

Moreover, according to Hardy's experiments [23], differences of k among different human beings are relatively much smaller than differences of K_0. If supposing k as a quasi-constant parameter for a group of subjects, then the *SBP* can be expressed with 3 variables and 4 constants:

$$SBP = C_3 \ln(PAT) + C_2 \ln(arm\_length) + \frac{1}{k}\ln(K_0) + C_0, \qquad \text{Eq. 3.7}$$

where C_3, C_2, C_0 are group constants and $C_2 > C_3$ (because the arm length always smaller than the real transit distance along arteries). Thus, the rest problem is how to evaluate K_0.

With constant k, K_0 mainly depends on the limiting value of the vessel volume $\underline{V_m}$ as in Eq. 2.25. A larger V_m corresponds with a larger K_0. The expansion limitation of the vessel tube, i.e. values of V_m, depends on the elastic properties of vessel all. It's not only subject-dependent, for example correlated with age, but also sensitive to changes of emotions, physical exercise and drug injection. Studies have shown that the shape of detected PPG waveform is affected by the hemodynamic properties of the vasculature including arterial elasticity [24][25][26][27][28]. Therefore, the PPG waveform might convey information related to K_0. If this "unknown" parameter from PPG is named X, Eq. 3.7 can be expressed as

$$SBP = C_3 \ln(PAT) + C_2 \ln(arm\_length) + C_1 X + C_0, \qquad \text{Eq. 3.8}$$

where C_3~C_0 are all group constants, and the item "C_1X" is used to substitute $\frac{1}{k}\ln(K_0)$. The form of "C_1X" is determined by whether the PPG waveform parameter X is determined by K_0 or the whole item of $\frac{1}{k}\ln(K_0)$. Therefore, "C_1X" and "$C_1 \ln(X)$" are both possible forms.

C_3~C_0 are calibrated by group regression method. The Eq. 3.8 will be trained by a

group of subjects at first and then be tested on another group with no overlap, of which the procedures are much similar with the method in Section 3.2.3. If it would like to be used as an individual approach, the items of $C_2 \ln(arm\_length)$ and C_0 merged together as an individual constant, i.e.

$$SBP = D_2 \ln(PAT) + D_1 X + D_0, \qquad \text{Eq. 3.9}$$

where D_2~D_0 are individual constant. As assuming k is generally constant in Eq. 3.6, D_2 and D_1 can be set as group constants while D_0 should be calculated by one cuff reading.

3.3.2. Selection of parameters from PPG waveform

The contour analysis of the photoplethysmography has been discussed for couples of years. Amongst dozen kinds of different definitions of PPG waveform parameters, those related to PPG rising time and dicrotic notch are the mostly reported to represent the arterial stiffness or elasticity of vessels. The PPG rising time is the time from the foot point to the peak of a PPG wave while the dicrotic notch is the acute drop between the highest Peak (main Peak) and the secondary peak.

In Zahedi's work, the rising time was a function of age according to both the experimental results and a modified Windkessel model [29]. The time interval between the secondary peak and the main Peak is found to be correlated with age and/or vascular diseases [30] and the position of the dicrotic notch is found to vary with physiological changes during exercise [31]. In my previous work [32], it has been attempted to use the amplitude ratio of the secondary peak to the main peak (RAS) to improve the one-cuff calibration of PAT-BP estimation. By using the RAS to represent the changes with exercise (as shown in Fig. 3.4), the estimation errors have been reduced roughly 3 mmHg. However, the main problem of parameters from dicrotic notch is that, sometimes the identification of dicrotic notch is quite difficult,

especially for aged subjects. For example, the PPG segment in Fig. 3.3 is acquired from a 65-year-old subject and its falling part from the main Peak is straight with no obviously notch.

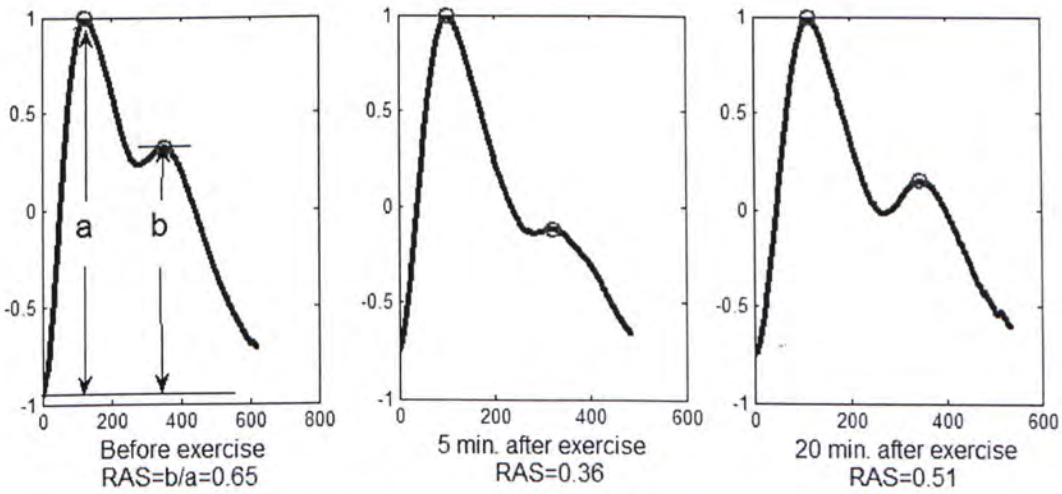

Fig. 3.4 changes of PPG dicrotic notch/secondary peak in different phases (before exercise, 5 min. after exercise and 20 min. after exercise)

In order to overcome the drawbacks of dicrotic notch, a new alternative parameter, Zero Crossing (ZX), has been proposed in this thesis. ZX derived from the waveform of PPG was used to represent the physiological condition of arteries. As indicated in Fig. 3.5, ZX is the number of zero points of the secondary derivative of PPG wave during the falling time of PPG in one heart cycle. According to the theory of convex optimization, whether negative or positive the second derivative of a function is will represent its convexity [33] so that the increase in ZX indicates that the fluctuation of the PPG signal is larger with more switches between convex and concave. Thus, ZX shows the reflection fluctuation property of arterial wall. Moreover, similar to the properties of dicrotic notch, ZX are also sensitively changed with physiological state variations, such as those caused by exercise (Fig. 3.6). This parameter was first defined by me in [34]. It is hoped that ZX be applied as the "unknown" PPG parameter X in Eq. 3.8.

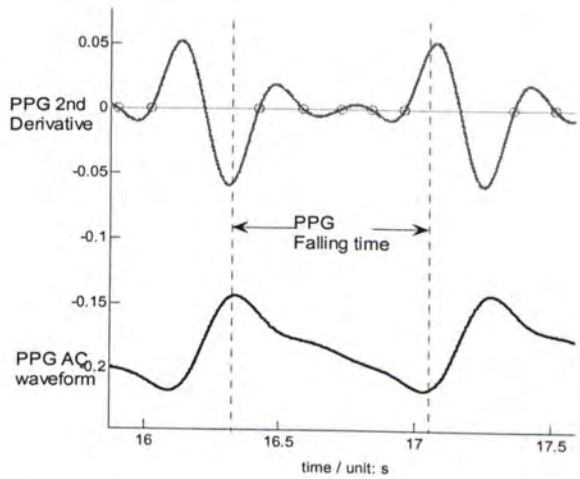

Fig. 3.5 The definition of Zero Crossing

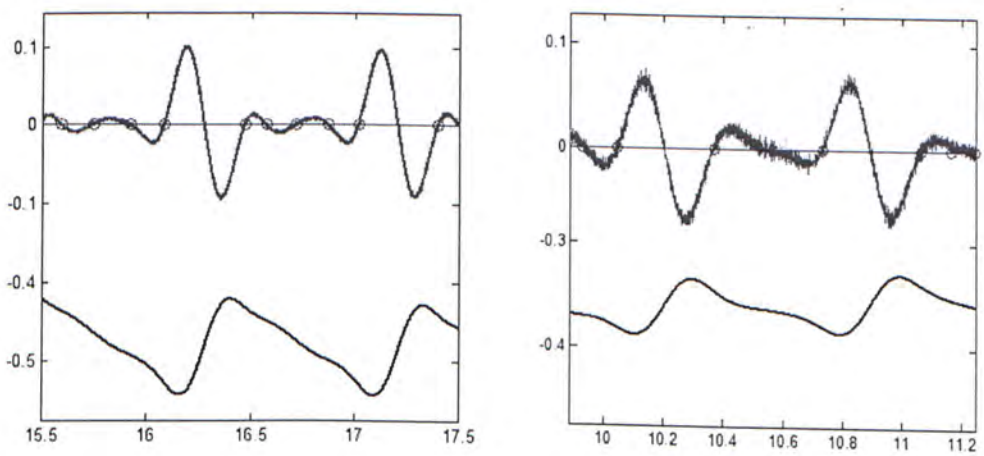

(a) (b)

Fig. 3.6 Variation of ZX in different physiological states: (a) rest; (b) after exercise.

Besides ZX, there are more PPG waveform parameters considered in this thesis. These parameters can be divided into three groups:

(1) Time parameters:

MaxP – time from the foot point to maximum of PPG wave;

L20 – time width of 20% of PPG wave amplitude;

L40 – time width of 40% of PPG wave amplitude;

L60 – time width of 60% of PPG wave amplitude;

L80 – time width of 80% of PPG wave amplitude;

DfrontP – time from PPG foot point to the 1st derivative wave maximum;

DbackP – time from PPG foot point to the 1st derivative wave minimum;

(2) Amplitude parameters:

MaxV – amplitude of maximum of PPG wave;

DfrontV – amplitude of PPG wave at the 1st derivative maximum point;

DbackV – amplitude of PPG wave at the 1st derivative minimum point;

ZX - the number of zero points of the 2nd derivative wave during the falling time of PPG wave;

(3) Area parameters:

Hrate – ratio of the area above 0.5×MaxV to the area below 0.5×MaxV;

Vrate – ratio of the area in front of MaxP to the area after MaxP;

2ndD_area – the absolute area under the normalized 2nd derivative wave.

Fig. 3.7 describes these possible waveform parameters of PPG. All these parameters will be tested which one can bring improvement to PAT-BP estimation as the parameter "X" in Eq. 3.8 or Eq. 3.9.

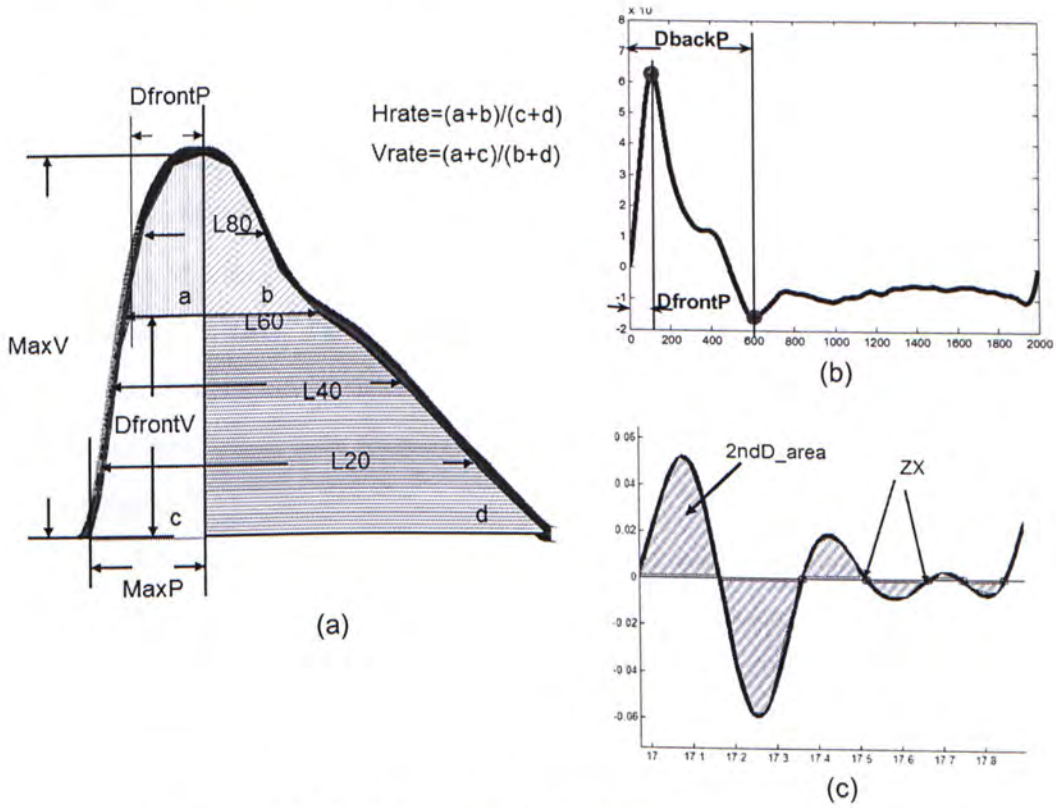

Fig. 3.7 Definition of PPG waveform parameters:
a) at AC wave; (b) at 1st derivative wave; (c) at 2nd derivative wave.

Reference

[1]. A Dictionary of Nursing. Oxford University Press, 2008. Oxford Reference Online.

[2]. http://en.wikipedia.org/wiki/Electrocardiography.

[3]. http://www.medis-de.com/index.php?option=com_content&task=view&id=38&Itemid=63&lang=en

[4]. J. Allen, "Photoplethysmography and its application in clinical physiological measurement," Physiological Measurement, 2007(28) pp.R1-R39.

[5]. Y. Yan, "A model-based motion-resistant method for noninvasive and continuous measurement of arterial blood pressure," PhD thesis, The Chinese University of Hong Kong, Hong Kong, 2005.

[6]. A. Hertzman, "The blood supply of various skin area as estimated by the photo-electric plethysmography," Am. J. Physiol, 1938(124) pp. 328-340.

[7]. V. Crabtree and P. Smith, "Physiological models of the human vasculature and photoplethysmography," 1st Electronic Systems and Control Division Research Mini-conference, Leicestershire, UK, 2003 pp.57-60.

[8]. W. Nichols and M. O'Rourke, "McDonald's blood flow in arteries – Theoretical, experimental and clinical principles," 5th edition, Oxford University Press Inc., 2005.

[9]. G. Marie, C. Lo, J. Jones, and D. Johnston, "The relationship between arterial blood pressure and pulse transit time during dynamic and static exercise," Psychophysiology, 1984(21) pp. 521-527.

[10]. L. Geddes, M. Voelz, C. Babbs, J. Bourland, and W. Tacker. "Pulse transit time as an indicator of arterial blood pressure," Psychophysiology, 1981(18) pp.71-74.

[11]. W. Chen, T. Kobayashi, S. Ichikawa, Y. Takeuchi, and T. Togawa."Continuous estimation of systolic blood pressure using the pulse arrival time and intermittent calibration," Med. & Biol. Eng. & Comput., 2000(38) pp. 569-574.

[12]. J. Lass, K.Meigas, D. Karai, R. Kattai, J. Kaik, and M. Rossmann, " Continuous blood pressure monitoring during exercise using pulse wave transit time measurement," in Proc. of the 26th Ann.Int. Conf. of the IEEE EMBS, San Francisco, USA, 2004, pp.2239-2242.

[13]. C. Chua and C. Heneghan, "Continuous Blood Pressure Monitoring using ECG and Finger Photoplethysmogram," in Proc. of the 28th Ann. Int. Conf. of the IEEE EMBS, New York City, USA, 2006, pp.5117-5120.

[14]. C. Poon and Y. Zhang, "Cuff-less and Noninvasive Measurements of Arterial Blood Pressure by Pulse Transit Time," in Proc. of the 27th Ann. Int. Conf. of the IEEE EMBS, Shanghai, China, 2005,

pp.5877-5880.

[15]. M. Wong, C. Poon, and Y. Zhang, "An Evaluation of the Cuffless Blood Pressure Estimation Based on Pulse Transit Time Technique: a Half Year Study on Normotensive Subjects," Cardiovasc. Eng. 2009(9) pp.32-38.

[16]. P. Shaltis, A. Reisner, H. Asada, "A hydrostatic pressure approach to cuffless blood pressure monitoring," in Proc. of the 26th Ann. Int. Conf. of the IEEE EMBS, San Francisco, USA, 2004, pp.2173-2176.

[17]. C. Poon, Y. Zhang, and Y. Liu, "Modeling of Pulse Transit Time under the Effects of Hydrostatic Pressure for Cuffless Blood Pressure Measurements," in Proc. of the 3rd IEEE-EMBS Int. Summer School and Symposium on Medical Devices and Biosensors, Boston, USA, 2006, pp.65-68.

[18]. D. McCombie, A. Reisner, and H. Asada, "Motion Based Adaptive Calibration of Pulse Transit Time Measurements to Arterial Blood Pressure for an Autonomous, Wearable Blood Pressure Monitor," in Proc. of the 30th Ann. Int. Conf. of the IEEE EMBS, Vancouver, Canada, pp.989-992.

[19]. C. Langenberg and R. Hardy, "Influence of height, leg and trunk length on pulse pressure, systolic and diastolic blood pressure," J. Hypertension, 2003(21) pp. 527-543.

[20]. S. Anderson and G. Cornelissen, "Age effects upon the harmonic structure of human blood pressure in clinical health," in Proc. 2nd Ann. IEEE Symposium on Computer-Based Medical Systems, Minneapolis, USA, 1989, pp. 238-243.

[21]. E. Park, B. Cho, S. Park, J. Lee, J. Lee, I. Kim, and S. Kim, "Continuous measurement of systolic blood pressure using the PTT and other parameters," in Proc. of the 27th Ann. Int. Conf. of the IEEE EMBS, Shanghai, China, 2005, pp.3555-3558.

[22]. Jung Yi Kim, Baek Hwan Cho, Soo Mi Im, Myoung Ju Jeon, In Young Kim, Sun I Kim, "Comparative study on artificial neural network with multiple regressions for continuous estimation of blood pressure," in Proc. of the 27th Ann. Int. Conf. of the IEEE EMBS, Shanghai, China, 2005, pp.6942-6945.

[23]. H. Hardy and R. Collins, "On the pressure-volume relationship in circulatory elements," Med. & Biol. Eng. & Comput., 1982(20) pp.565-570.

[24]. A. Challoner, "Photoelectric plethysmography for estimating coetaneous blood flow," Noninvasive Physiological Measurements, 1979(1) pp. 127-151.

[25]. J. Spigulis, G. Venckus, and M. Ozols, "Optical sensing for early cardiovascular diagnostics," Proc. SPIE, 2000(3911) pp. 27-31.

[26]. J. Spigulis, I. Kukulis, E. Fridenberga, and G. Venckus, "Potential of advanced

photoplethysmography sensing for non-invasive vascular diagnostics and early screening," Proc. SPIE, 2002(4625) pp. 38-43.

[27]. I. Hlimonenko, K. Meigas, and R. Vahisalu, "Waveform analysis of peripheral pulse wave detected in the fingertip with photoplethysmograph," Measurement Science Review, 2003(3) pp. 49-52.

[28]. J. Weinman, A. Hayat, and G. Raviv, "Reflection photoplethysmography of arterial blood volume pulses," Med. Biol. Eng. Comput., 1977(15) pp. 22-31.

[29]. E. Zahedi, K. Chellappan, M. Alauddin, M. Ali and H. Singh, "Analysis of the Effect of Ageing on Rising Edge Characteristics of the Photoplethysmogram using a Modified Windkessel Model," Cardiovasc Eng, 2007(7) pp.172–181.

[30]. S. Millasseau, J. Ritter, K Takazawa and P. Chowienczyk, "Contour analysis of the photoplethysmographic pulse measured at the finger," J. Hypertension 2006 (24) pp.1449-1456.

[31]. L. Xu, K. Wang, L. Wang and N. Li, " Pulse Contour Variability Before and After Exercise," in Proc. of the 19th IEEE Symposium on Computer-Based Medical Systems, 2006.

[32]. W. Gu, C. Poon and Y. Zhang, "A novel parameter from PPG dicrotic notch for estimation of systolic blood pressure using pulse transit time," in Proc. of the 5th IEEE-EMBS Int. Summer School and Symposium on Medical Devices and Biosensors, Hong Kong, 2008, pp.86-88.

[33]. S. Boyd and L. Vandenberghe, "Convex optimization," Cambridge University Press, 2004, chapter 3: pp.67-126.

[34]. W. Gu, C. Poon, M. Sy, H. Leung, Y. Liang, and Y. Zhang, "A h-Shirt-Based Body Sensor Network for Cuffless Calibration and Estimation of Arterial Blood Pressure," in Proc. 6th Int. workshop on Wearable and Implantable Body Sensor Network, Berkeley, USA, 2009, pp.151-155.

4. Cuffless calibration approach using PPG waveform parameter for PAT-BP estimation

4.1. Introduction

In order to evaluate the efficiency of the estimation equation Eq.3.8 in chapter 3, three experiments were conducted on a total number of 35 subjects covering a period of more than a half year.

4.2. Experiment I: young group in sitting position including rest and after exercise states

12 healthy subjects, including 6 males and 6 females, aged 23-30 years, participated in Experiment I. The experiment was conducted in May 2008.

4.2.1. Experiment protocol

Self-designed acquisition equipment was used to collect ECG and PPG simultaneously from finger tips of the subjects. Both kinds of signals were recorded for 45s in each trial at sampling rate of 1 kHz with the DATAQ instrument WINDAQ. An experienced nurse was invited to measure BP using a mercury sphygmomanometer by the auscultative method. An automatic BP machine (OMRON, Model HEM-907, Japan) was connected to the mercury sphygmomanometer with a Y-tube such that BP references can be obtained simultaneously by the nurse and from the oscillometric device. Exercises were implemented on a treadmill (Precor, Model C956, USA).

Each subject was asked to sit in a comfortable position on a chair and rest for 3

minutes while the operator measured the arm length of the subject from his/her scapula to index finger by a measuring tape. Reference BP was then measured every 2 minutes for four times. Between two cuff readings, ECG and PPG were recorded for 45 seconds. Subjects were then instructed to run on the treadmill (Precor, Model C956, USA) at 8 km/h for 3 minutes. After running, another four sets of BP readings and 3 sets of signal recordings were obtained.

4.2.2. Data Analysis

Since one dataset of a subject recorded before exercise was missing due to technical failure, a total of 71 datasets were collected from this experiment. Each dataset consisted of the averaged PAT measured from 45 seconds of ECG and PPG and the averaged BP of four cuff readings, two auscultative and two oscillometric readings measured before and after the signal recording, as the reference.

The recorded signals were analyzed offline using MATLAB 7.0.1. In order to calculate PAT and characteristic parameters from PPG waveform, some characteristic points on PPG and ECG signals should be recognized in previous.

The ECG signal was filtered by a band-pass linear phase filter using Hamming window of 400 orders (cut-off frequency is from 0.5 Hz to 50 Hz) in previous. The first derivative of filtered ECG was calculated, of which peaks in each heart cycle was located by an automatic threshold. According to these first derivative peaks, the R-peaks of raw ECG signals were searched as the maximum amplitude within 50ms of each first derivative peak. This algorithm can still recognize R-peak when the base line of ECG is fluctuant (Fig. 4.1).

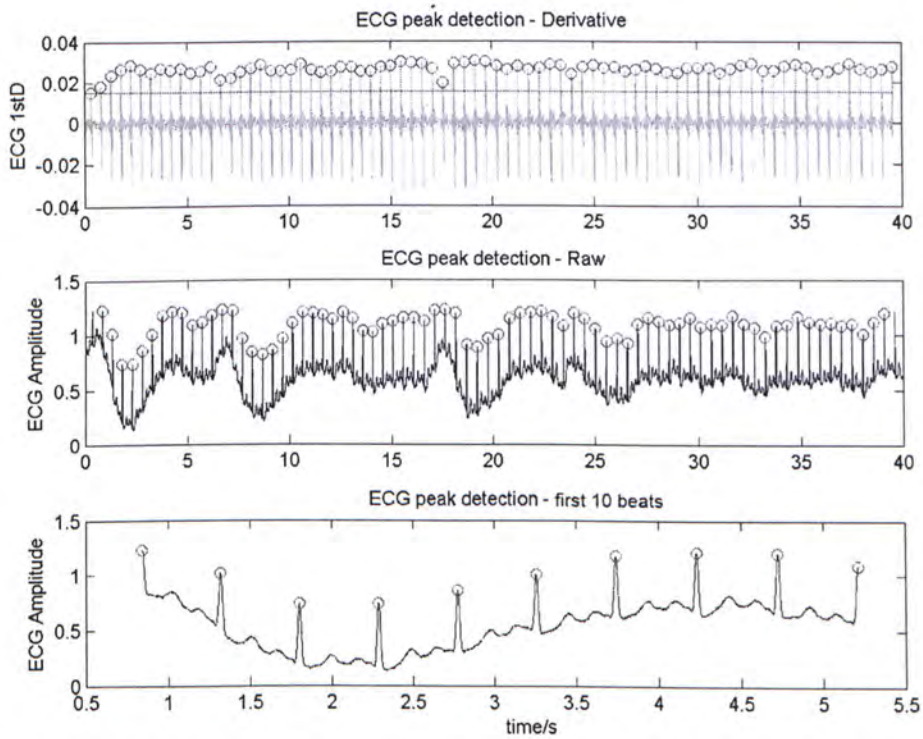

Fig. 4.1 An example R-peak detection of fluctuant ECG: top is the filtered first derivative ECG; middle is raw ECG with R-peak recognition; bottom is the first ten beats of the upper ECG.

The PPG signals were filtered by a linear filter using Hamming window of 400 orders (cut-off frequency is from 0.5 Hz to 20 Hz), as in Fig. 4.2. According to the position of R-peaks of simultaneous ECG, PPG signals were segmented. The PPG peak is defined as the point with the maximum amplitude in one heart cycle as well the first derivative point is the point of maximum of derivative signal. The on-set point, which is also called the foot point of PPG, is defined as the lowest point around the crossing of the raw PPG waveform and the extension line of PPG peak and first derivative peak (Fig. 4.3). Then, the PPG signal was differentiated twice to get its second derivative waves and the point across the zero line was counted.

Based on all these characteristic points for both ECG and PPG, PAT and every PPG waveform parameters are calculated as their definition in Section 3.3.2.

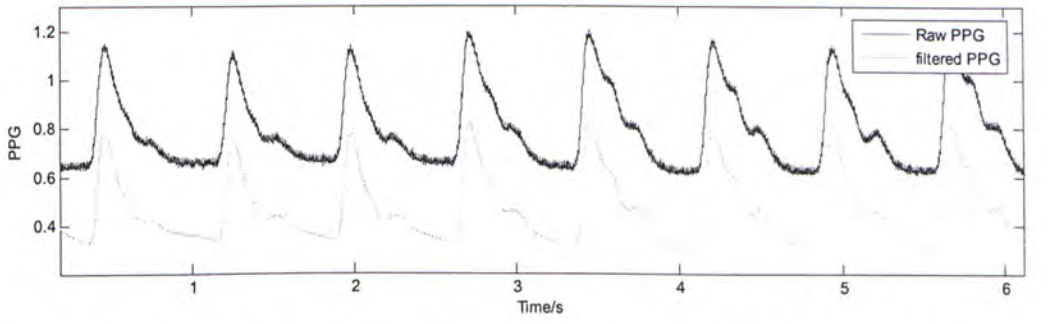

Fig. 4.2 Comparison of raw and filtered PPG with 0.5~20Hz band-pass filter

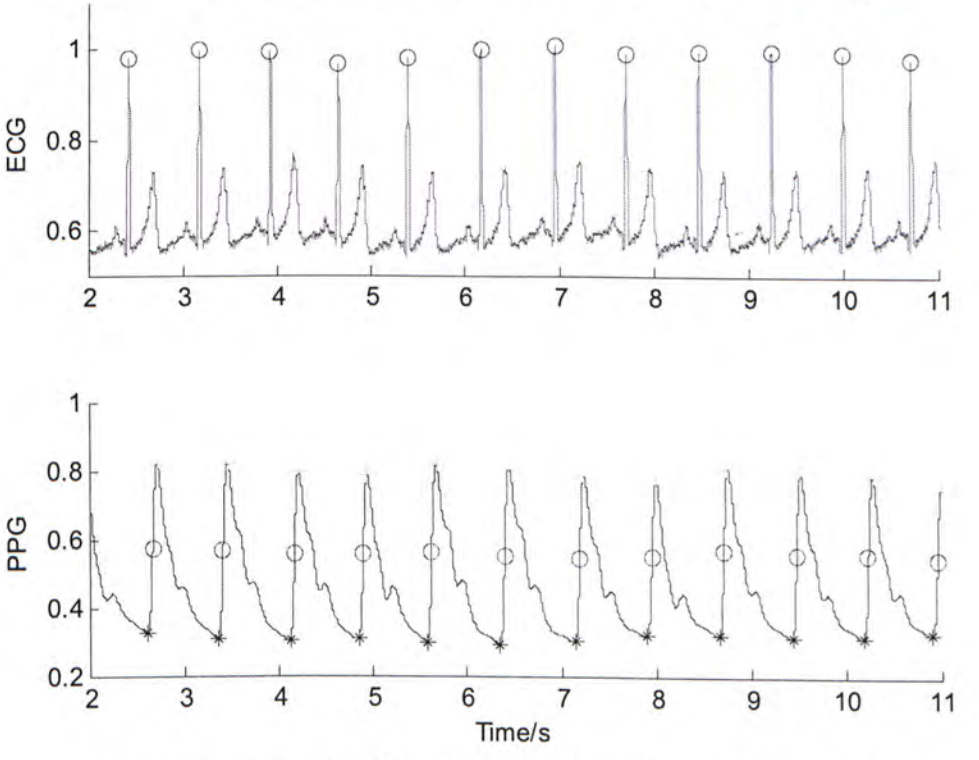

Fig. 4.3 PPG peak, 1st Derivative peak and foot point detection

4.2.3. Experiment results

Individual correlation between SBP, PAT and ZX: As shown in Table 4.1, the mean correlation of all subjects was -0.955 between PAT and SBP and -0.841 between ZX and SBP. However, the global correlations were not as high as the individual ones, global correlations of SBP-PAT and SBP-ZX were -0.563 and 0.600 respectively.

Table 4.1 Correlation of PAT and ZX with SBP

Subject	PAT	ZX
a01	-0.964	-0.836
a02	-0.902	-0.680
a03	-0.977	-0.750
a04	-0.993	-0.887
a05	-0.912	-0.943
a06	-0.996	-0.940
a07	-0.936	-0.885
a08	-0.934	-0.866
a09	-0.977	-0.940
a10	-0.909	-0.947
a11	-0.994	-0.946
a12	-0.972	-0.471
Mean	-0.955	-0.841
Global	-0.563	-0.600

Group regression results: The standard deviation (SD) of SBP of the 12 subjects was 17.0 mmHg. If we set C_2 and C_1 in Eq. 3.8 to zero, the root-mean-square error (RMSE) of regression errors and adjusted R^2 were 14.0 mmHg and 0.311, respectively, as shown in Fig. 4.4(a) (P-value of $C_3 < 0.001$). If only C_1 was set to zero, RMSE of the regression reduced to 8.2 mmHg, and adjusted R^2 was 0.761 (P-values of C_3 and $C_2 < 0.001$ and P-value of $C_0 < 0.05$). When *ZX* and *arm length* were both introduced into the regression, the RMSE was 7.0 mmHg, and adjusted R^2 was 0.821, as shown in Fig. 4.4(b) (P-values of C_3, C_2, C_1, and $C_0 < 0.001$).

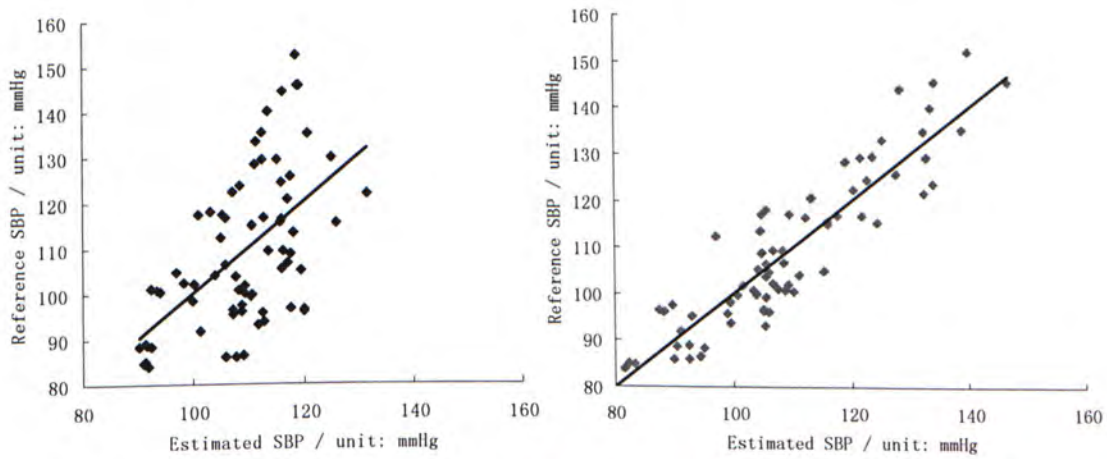

Fig. 4.4 Regression results of Experiment I: (a) only with PAT; (b) with PAT, arm length, ZX [3]

Estimation results: In order to test the accuracy of the algorithm, the subject pool was randomly divided into two groups with equal numbers. By regression analysis, data of one group were used to obtain C_3, C_2, C_1 and C_0, which were then used for estimating BP for the other group. Three attempts were made and the results were shown in Table 4.2.

Table 4.2 Estimation results by Eq. 3.8

Attempt	SD of reference SBP (Estimated group)	RMSE of regression (6 subjects)	Estimation error (6 subjects)
1	16.9	6.7	1.5±8.0
2	17.6	7.0	-1.1±8.2
3	18.4	6.1	-2.2±7.2

Unit: mmHg

4.3. Experiment II: over-month observation using wearable device in sitting position

In Experiment I, blood pressure can be estimated by PAT, arm length and ZX with constant C_3~C_0 within a regression RMSE of 7.0 mmHg and an estimation SD error of 8.5 mmHg. In order to fatherly verifying the efficiency of this cuffless approach on different subjects and by using wearable device, Experiment II was conducted on 21 healthy subjects, including 11 males and 10 females, aged 21-35 years.

None of these 21 subjects had participated in Experiment I. And 9 of them (4 males and 5 females) approached the same experiment protocol in both February 2009 and April 2009; 11 subjects (6 males and 5 females) took this experiment only in April; and there is a male subject who only attended the experiment in February. In addition, an h-shirt-based body sensor network device was tested in this experiment and used for signal acquisition.

4.3.1. Body sensor network for blood pressure estimation

Based on the earlier work of my research group on h-Shirt [1] and hybrid-BSN [2], a cuff-less system was designed for measuring BP [3]. In this system, ECG was collected by e-textile sewed on a jacket and PPG by a pair of infrared emitter and sensor embedded in a module wearable on the forearm of the subject. A MCU and a Bluetooth module were used for digitizing signals and wirelessly transmitting them to a computer respectively. Continuous ECG and PPG and parameters such as SBP, DBP and PAT can be calculated and displayed on screen, as shown in Fig. 4.5(a).

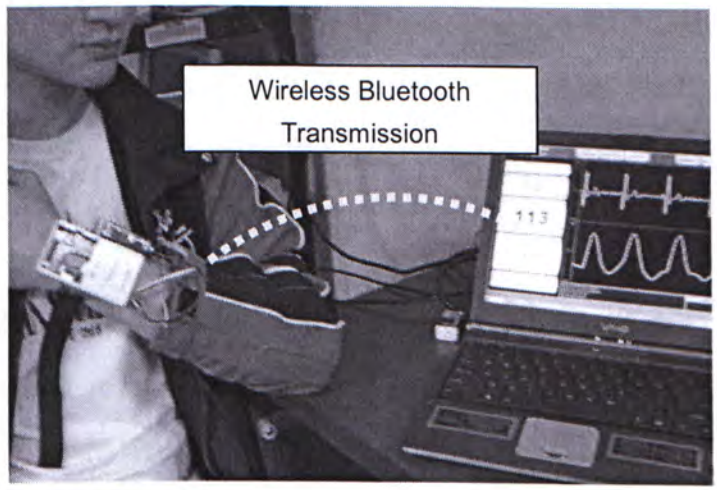

(a)

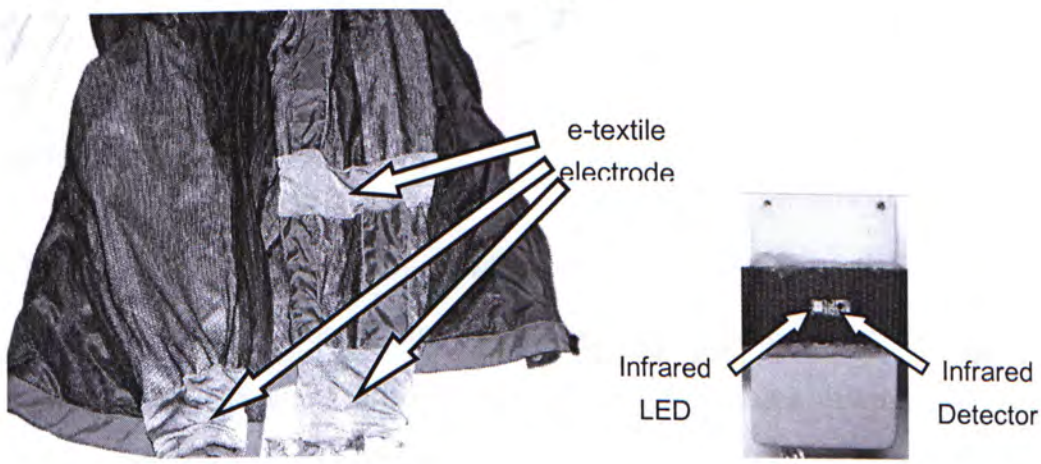

(b) (c)

Fig. 4.5 Wireless body sensor network system for blood pressure monitoring: (a) general view of the cuffless and wireless body sensor network; (b) E-textile materials sewed inside of the jacket for collecting ECG; (c) Placement of the PPG sensor. [3]

As shown in Fig. 4.5(b), two pieces of e-textile material were used as ECG electrodes and sewed inside the cuffs of the jacket, while another piece sewed inside a sleeve was used as the reference to avoid noise induced by motion. Fig. 4.5(c) shows the module with the PPG sensor embedded on the bottom. By wrapping the module around the forearm of the subject, PPG can be collected.

4.3.2. Experiment protocol and data collection

Each subject rested for 3 minutes while the operator measured the arm length of a subject from his/her scapula to the PPG sensor. Cuff BP were then measured every 2 minutes for four times by the automatic BP machine (OMRON, Model HEM-907, Japan). In between two cuff measurements, ECG and PPG were collected simultaneously for 1 minute using the body sensor network system described in section 4.3.1.

A total of 90 datasets were collected in this experiment from Feb to April, amongst which 30 datasets were recorded in Feb and the other 60 ones were in April. Each set of data consisted of the averaged PAT of the 1-minute recording and the averaged of the two cuff blood pressure measured before and after signal recording. The signal characteristic procedures were similar with the algorithm described in section 4.2.2.

4.3.3. Experiment results

Using constant coefficients C_3~C_0 which were calculated from the regression result (section 4.2.3) of 12 subjects in Experiment I, blood pressure was estimated as the format of Eq. 3.8 under different conditions. The detailed equation with specific values of C_3~C_0 was as following:

$$SBP = -79.8 \times \ln(PAT) + 155.7 \times \ln(arm\_length) - 5.5 \times ZX + 77.6 \quad \text{Eq. 4.1}$$

where units of *PAT, arm_length* and *SBP* were m/s, m, and mmHg respectively. Since the placement of sensors and circuit design were different for the two experiments, PAT was adjusted for a group bias. As contrasts, estimation results with only PAT, and with PAT and arm length were calculated as well. Table 4.3 gives a summary of these estimation results.

Table 4.3 Estimation results of Experiment II by using Eq. 4.1

Experiment Date	No. of Subjects	No. of datasets	SD of SBP (mmHg)	Estimation Error (mmHg)		
				Condition I*	Condition II*	Condition III*
Feb. & Apr.	21 subjects (all)	90	13.6	1.2±6.6	3.1±9.2	-0.5±13.7
Feb.	10 subjects (all in Feb)	30	13.3	1.0±6.1	-1.4±8.8	-3.0±12.6
Apr.	20 subjects (all in April)	60	13.6	1.4±6.9	5.3±8.7	0.7±14.2
Feb.	9 subjects** (tested twice)	27	13.9	0.8±6.4	-2.4±8.6	-3.6±13.1
Apr.	9 subjects** (tested twice)	27	15.3	2.4±7.5	5.9±9.0	1.5±14.0

* Condition I: C_3, C_2, C_1 and $C_0 \neq 0$, i.e. using Eq. 4.1
Condition II: $C_1 = 0$; C_3, C_2 and $C_0 \neq 0$;
Condition III: C_2 and $C_1 = 0$; C_3, and $C_0 \neq 0$.

** These nine subjects participated in both the experiments in February and April.

4.4. Experiment III: contactless monitoring in supine position

The results of Experiment I and II have shown the success of the cuffless calibration approach for PAT-BP estimation in sitting position and using wearable device. The purpose of Experiment III is to evaluate qualities of the signals acquired from a contactless system and to implement the calibration and estimation method in supine position. Different from the contact system and wearable system used in previous experiments, the contactless system dose not require users to put on or get in contact with any sensors so that its design has a promising future of the implementation for

over-night undisturbed monitoring.

11 healthy subjects, including 5 males and 6 females, aged 23-35 years, participated in this experiment, 9 of which (4 males) used to participate in Experiment II and the other two of which never participated in both Experiment I and II.

4.4.1. The design of the contactless system

The contactless system was designed on a soft and flexible sleeping cushion (h-Cushion[4]) that is to be placed in between the mattress and bed sheet. As shown in Fig. 4.6, e-textile electrodes and a pair of photo emitter and sensor were embedded on h-Cushion for capturing ECG and PPG by a contactless approach[5].

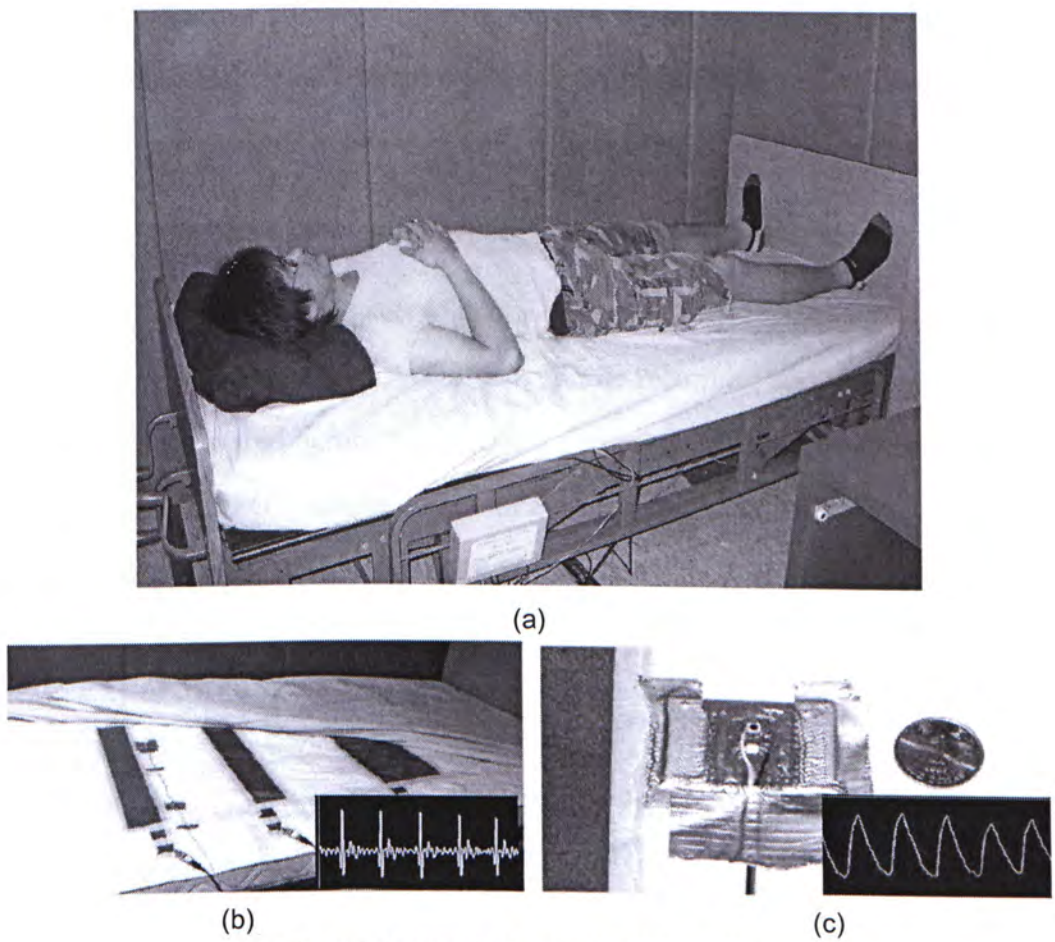

Fig. 4.6 Design of the contactless system:
(a) appearance, (b) e-textile electrodes, and (c) LED and photodiode pair. [5]

In this novel system, a PPG sensor board was carefully designed so that it is comfortable to be slept on while being able to maintain sufficient contacting pressure against the user for capturing the pulse from the back of the user. A pair of narrow-band infrared LED and photodiode was selected to reduce the interference of visible light from surrounding environment.

4.4.2. Experiment protocol and data collection

Each subject was asked to lie on the contactless system described in Section 4.4.1 for 6 minutes. For references, ECG and PPG were simultaneously collected by sensors that were clipped onto the fingertips and forearms of the subjects, i.e. by a contact approach. An automatic BP machine (OMRON, Model HEM-907, Japan) was used to measure reference BP on the left upper arm of the subject at the beginning of signal recording and every 2 minutes afterwards. Including a cuff reading taken after the 6-minute recording, a total of four cuff readings were measured from each subject.

From the above recording, 33 sets of data were extracted for each system. Each set of data consisted of the averaged PAT of a 1-minute recording and the averaged of the two cuff BPs measured before and after the recording. The distances from subject's shoulder to the PPG sensors were measured after data recording. The signal characteristic procedures were similar with the algorithm described in section 4.2.2.

4.4.3. Experiment results

Fig. 4.7 shows a typical segment of ECG and PPG recorded simultaneously by the contact and contactless systems.

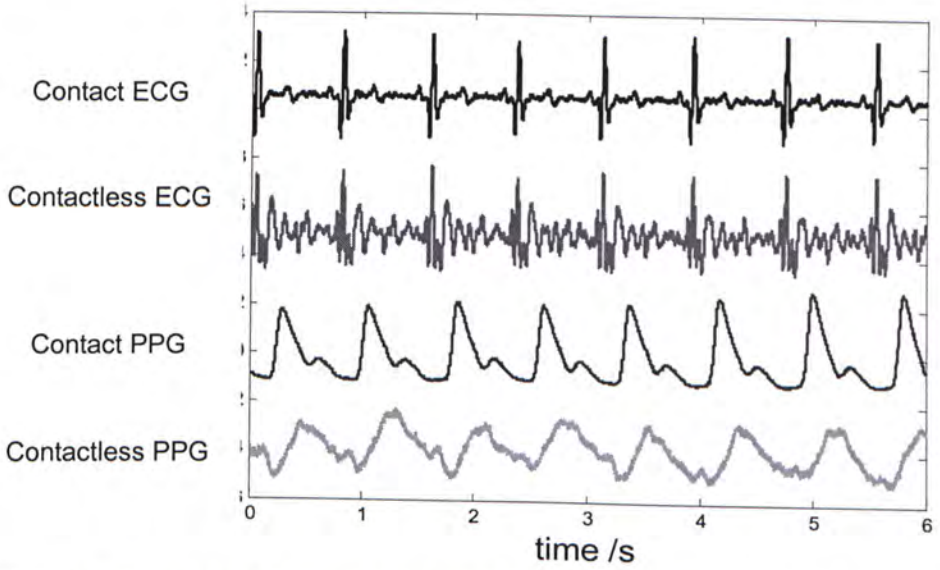

Fig. 4.7 A typical recording of the signals obtained by the contact and contactless systems

SBP of the 11 subjects in Experiment I ranged from 86 mmHg to 117 mmHg with a SD of 9.3 mmHg. Table 4.4 shows the regression results of SBP by Eq. 3.8 for both the contactless and contact systems.

Table 4.4 Regression results by using signals from contact and contactless systems

System	RMSE of Regression	P-value of variable coefficients			
		C_3	C_2	C_1	C_0
Contactless	7.1 mmHg	<0.05	<0.05	<0.05	0.091
Contact	7.4 mmHg	0.424	<0.05	0.568	<0.05

For the 9 subjects who have participated in both Experiment II and Experiment III, their SBP were 101.3±9.8 mmHg and 111.6±13.4 mmHg when measured at supine and sitting postures respectively. Using regression analysis on Eq. 3.8, the RMSEs of estimations were 7.9 mmHg and 5.5 mmHg for the supine and sitting postures respectively (see Table 4.5). Fig. 4.8 compares the regression results in supine and sitting postures.

Table 4.5 regression results in different postures

Posture	RMSE of Regression	Variation of Parameters		
		SBP (mmHg)	PAT (ms)	ZX
Supine (Experiment III)	7.9 mmHg	101.3±9.8	197±19	5.1±0.6
Sitting (Experiment II)	5.5 mmHg	111.6±13.4	228±17	4.4±0.6

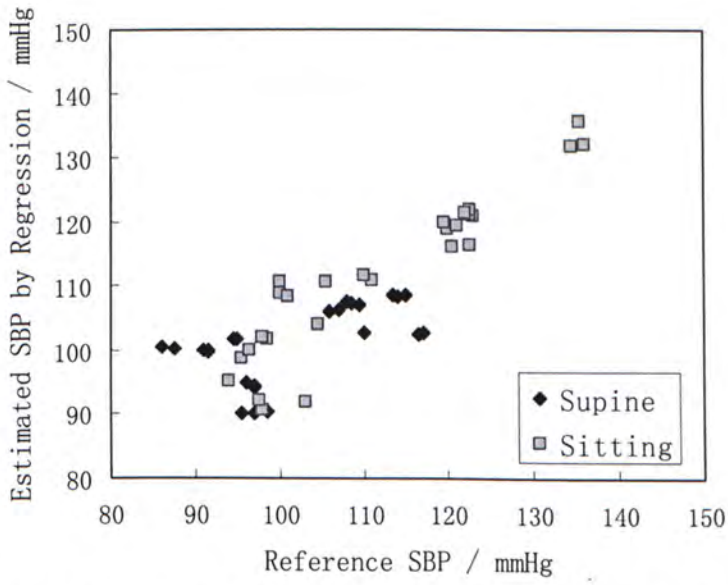

Fig. 4.8 Estimation of SBP by regression at different postures [5]

4.5. Discussion

4.5.1. Discussion of Experiments I and II

The experiment results of Experiment I show that PAT correlated with SBP individually but not as a group. When only PAT was used with some constant coefficients for SBP estimation, the results were poor (regression analysis resulted in SD=14.0 mmHg for Experiment I and the estimation differed from the reference by -0.5±13.7 mmHg for Experiment II). Thus, the results suggest that the coefficients for PAT-BP estimation equation are individual dependent.

The proposed cuffless calibration approach by group regression with PPG waveform parameters is developed based on measuring the time and distance travelled by the pulse and physiological properties of arterial wall. Its advantage is that no extra sensor or inflatable cuffs should be included and the coefficients in Eq. 3.8 are group determined. This new method has been successfully applied on Experiment I and Experiment II, involving a total of 33 healthy young subjects in sitting position.

In Experiment I, the regression result for all 12 subjects was SD=7.0 mmHg. When the same regression coefficients were used in Experiment II by Eq. 4.1, the overall estimation result of 21 subjects was 1.2±6.6 mmHg. It should be emphasized that none of the subjects in Experiment II had participated in Experiment I and the errors of estimation have no obvious relationship with the values of SBP as shown in Fig. 4.9. Therefore, these results were not achieved by chance.

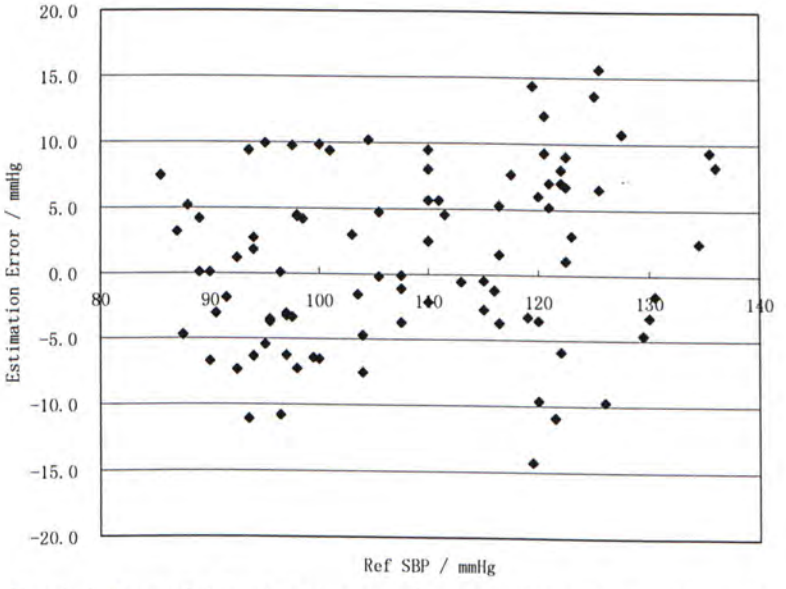

Fig. 4.9 Error distribution versus reference SBP in Experiment II.

From the view of modelling: According to L. Dahn's in-vivo experiment in human leg arteries, the parameters k and K_0 valued as the following Table 4.6 [6]:

Table 4.6 In-vivo experimental values of the volume-pressure parameters

	$h=\ln 2/k$ (mmHg)	k ($mmHg^{-1}$)	$2/k$ (mmHg)	K_0	$(1/k)*(\ln K_0)$ (mmHg)
Human 1	24.3	0.0285	70.1	0.657	-14.7
Human 2	20.9	0.0332	60.3	0.545	-18.3
Human 3	21.8	0.0318	62.9	0.370	-31.3

In Eq. 4.1, the value of C_3 is quite closed to the values of $2/k$ above while the range of item C_1*ZX is just in the variation range of $(1/k)*(\ln K_0)$ considering the normal range of ZX is from 2~6.

From the view of each added parameters: The introduction of arm length brings significant improvement to the estimation, reducing the SD of regression error from 14.0 mmHg to 8.2 mmHg in Experiment I and the estimation error from -0.5±13.7 mmHg to -3.1±9.2 mmHg in Experiment II. Moreover, the new parameter ZX, derived from the PPG waveform, further improved the BP estimation.

From the view of physiological state changes: Experiment I included exercise procedures so that 31 out of 72 datasets were measured after exercise. We have randomly selected data of 6 subjects in Experiment I for regression to estimate BP for the other 6 subjects and found that the SD of estimation errors were around 7.2-8.2 mmHg with small absolute mean errors around 2 mmHg.

From the view of monitoring overtime: There are nine subjects included Experiment II at both February and April. The BP estimation errors of these two measurement period were comparative as 0.8±6.4 mmHg and 2.4±7.5 mmHg respectively.

4.5.2. Discussion of Experiments II and III

In Experiment II, a wearable device based on body sensor networks were successfully used for data acquisition and BP estimation. This technology can be implemented for mobile monitoring during day time. In Experiment III, a contactless system for BP estimation has been tested on a sleeping bed. The results showed that the quality of ECG and PPG obtained from the back of the subject by a contactless approach are generally sufficient for estimating a robust PAT for the measurement of BP (Fig. 4.7). This technology is suitable for applying to nighttime monitoring of BP as it does not disturb the user's sleep.

However, the calibration and estimation results of Experiment III showed that the cuffless method of Eq. 3.8 cannot be directly applied to estimate SBP in supine position. Regression results from both contact and contactless systems are larger than

7 mmHg while the standard variation of SBP was only 9.3 mmHg.

As mentioned before, PAT consists of PEP and PTT. According to Bramwell-Hill's model, PTT is negatively correlated with BP while PEP is considered as a negligible constant. Therefore, PAT should increase from sitting up to lying down when BP of the subject decreased. However, comparing the results of Experiments II and II, both PAT and BP decreased after the change of posture. One possible explanation of this phenomenon is that PEP variation with posture change should be accounted for and this kind of PEP variation is subject-specific [7]. Nevertheless, this could not fully explain the phenomenon. As shown in Table 4.5 and Fig. 4.8, the SD of differences between the reference BP and BP estimated by regression is considerably larger when measured at supine than at sitting, indicating new compensation factors must be considered [5]. Further investigation should be conducted to understand the difference of BP estimation at different postures.

4.5.3. Conclusion

As considered these results from each aspect above all, it can be concluded that this new cuffless calibration of SBP estimation by Eq. 3.8 is consistent with the deduced theories in Chapter 2 and 3. Its efficiency for young healthy subjects with measurement in sitting position had been proved in both Experiments I and Experiment II. Even when physiological changes by exercise and long-term factors are included, it can still work well.

Compared this method with other existing cuffless calibration methods described in Chapter 3, the proposed method not only has better estimation accuracy, but also is much easier to be operated than the hydrostatic method does and has more theoretical support than the common regression method does (Table 4.7).

Table 4.7 The comparison among cuffless calibration methods of PAT-BP estimation

Calibration approach	Hydrostatic pressure (Section 3.2.2)	Group regression (Section 3.2.3)	**Proposed cuffless method**
Type of estimated BP	MBP	SBP	SBP
range of reference (mean±SD mmHg)	92.5±9.6	113.4±8.0	108.3±13.6
No. of subjects	8	45	33
No. of Datasets for estimation test	8	40	90
Estimation Error (Mean±SD mmHg)	1.3±7.1	5.8±4.2	1.2±6.6
Extra information required	Accelerometer External pressure sensor Extra PPG sensor	Arm length weight	Arm length PPG waveform

However, this method cannot be directly applied for estimation in supine position, indicating that new compensation factors should be considered. Therefore, further investigation should be conducted to understand the difference of BP estimation at different postures and to find an alternative way for BP estimation in supine position.

Reference

[1]. Y. Zhang, C. Poon, C. Chan, M. Tsang, and K. Wu, "A health-shirt using e-textile materials for the continuous and cuffless monitoring of arterial blood pressure", in Proc. 3rd IEEE-EMBS Int. Summer School and Sym. on Medical Devices and Biosensors, Cambridge, MA, U.S.A., 4-6 Sept., 2006, pp. 86-89.

[2]. C. Chan, C. Poon, R. Wong and Y. Zhang, "A hybrid body sensor network for continuous and long-term measurement of arterial blood pressure", in Proc. 4th IEEE-EMBS Int. Summer School and Sym. on Medical Devices and Biosensors, Cambridge, U.K., 19-22 Aug, 2007.

[3]. W. Gu, C. Poon, M. Sy, H. Leung, Y. Liang, and Y. Zhang, "A h-Shirt-Based Body Sensor Network for Cuffless Calibration and Estimation of Arterial Blood Pressure," in Proc. 6th Int. workshop on Wearable and Implantable Body Sensor Network, Berkeley, USA, 2009, pp.151-155.

[4]. K. Wu and Y. Zhang, "Contactless and Continuous Monitoring of Heart Electric Activities through Clothes on a Sleeping Bed," in Proc. 5th Int. Conf. Technology and Applications in Biomedicine, Shenzhen China, 2008, pp. 282-285.

[5]. W. Gu, C. Poon, H. Leung, M. Sy, M. Wong and Y. Zhang, "A Novel Method for the Contactless and Continuous Measurement of Arterial Blood Pressure on a Sleeping Bed," in Proc. 31st Ann. Int.

Conf. of IEEE-EBMS, Minneapolis, USA, 2009, pp. 6084-6086.

[6]. L. Dahn, B. Johson, and R. Nilson, "Plethysmographic in vivo determination of the elastic properties of arteries in man," J. Appl. Physiol. 1970(28) pp.328-332.

[7]. J. Muehlsteff, X. Aubert, and G. Morren, "Continuous Cuff-less Blood Pressure Monitoring based on the Pulse Arrival Time Approach: The Impact of Posture," in *P*roc.30th Annual Int. IEEE EMBS Conf., Vancouver, Canada, 2008, pp.1691-1694.

5. Cuff-based calibration approach for BP estimation in supine position

5.1. Introduction

In order to further investigate the PAT-BP estimation in supine position, two similar experiments including exercise procedures were conducted in both lab environment and in Prince of Wales Hospital with comparison of age and diseases. Since the cuffless calibration was not efficient in supine position in Experiment III, the alternative Eq. 3.9, which is suitable for cuff-based calibration, were evaluated in this chapter for improving the estimation results.

20 young and healthy subjects, including 9 males and 11 females, aged 22-35 years, participated in Experiment IV in Feb 2009. 20 patients including 16 males and 4 females, aged 49~83 years, participated in Experiment V from Feb to April, 10 out of whom used to have a heart failure while 8 have chronic diseases.

5.2. Experiment protocol

For the aim of easier comparison with each other, the protocols of Experiment IV and V were similar. Experiment V was designed and co-operated with the Cardiology Department of Prince of Wales Hospital.

5.2.1. Experiment IV: exercise experiment in supine position in lab

Self-designed acquisition equipment was used to collect PPG simultaneously from the left index finger tip and the right ear of the subjects. ECG signal was collected by the commercial ICG machine (Physioflow® Version 5) from the chest of the subjects. As a comparison, continuous reconstructed brachial blood pressure was estimated by

the Finometer (Finapres® Serial No.: FM.1.MU.281) according to the cuff pressure from left middle finger tip. All these signals were simultaneously recorded during the experiment at sampling rate of 1 kHz with the DATAQ instrument WINDAQ. An experienced nurse was invited to measure BP from subject's right upper arm by using the auscultative method with a mercury sphygmomanometer. Exercises were implemented on a bicycle (X2FIT®, Taiwan), of which the working load can be manually controlled (Fig. 5.1).

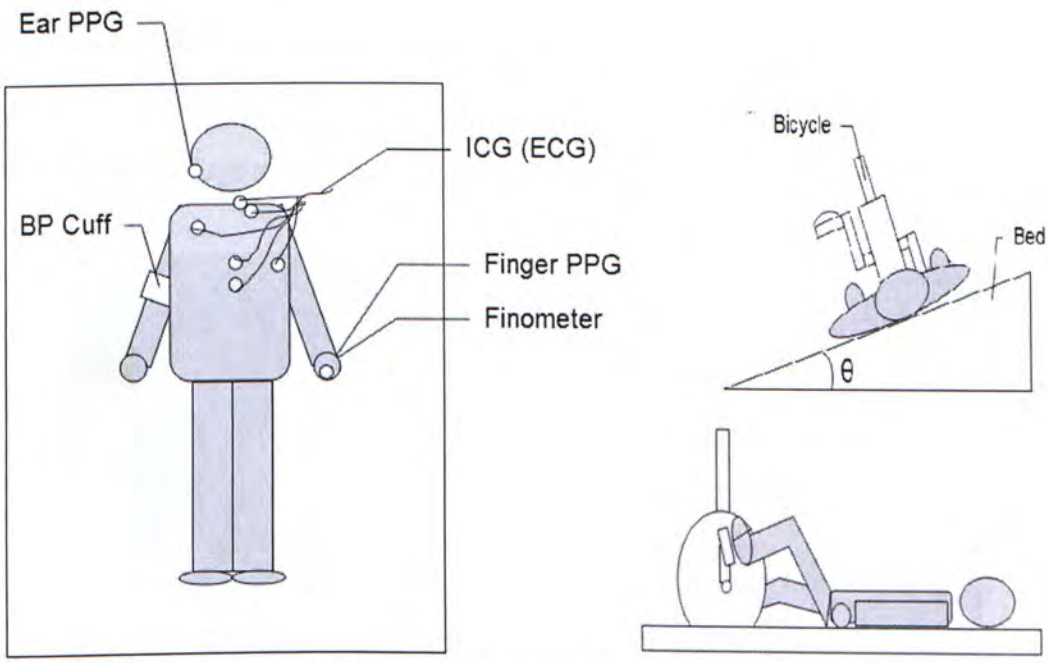

Fig. 5.1. General view of equipment settings of Experiment IV

Each subject was asked to lie on his/her back on a mattress which had an angle around 15° with the horizontal line. Their hands naturally put on the sides of the body. With wearing all the sensors and cuffs of PPG, ECG, Finometer and sphygmomanometer, each subject should complete an 18-minute experiment process, including 4 minutes lying quietly, 6 minutes bicycle exercise, 6 minutes lying quietly and 2 minutes sitting. The work load of the exercise part is 25w, 50w and 75w for each 2 minutes respectively. During this 18-minute experiment, PPG, ECG and Finometer signals were continuously recorded and cuff BP values were read every 2 minutes.

5.2.2. Experiment V: exercise experiment in supine position in PWH

The same PPG, ICG and Finometer equipments of Experiment IV were used in Experiment V with similar sensor location, except the finger cuff of the Finometer were moved to the right middle finger tip. An additional 12-lead ECG machine integrated with an automatic BP machine (BP-Monitor, Sun tech, USA) was used for detecting cardiac electric signals and BP readings as a part of requirements from the hospital. A Y-tube was used to connect the sphygmomanometer and the oscillometric device so that BP references were obtained simultaneously by the nurse and the automatic machine. A bicycle with adjustable work load (Echo Cardiac Stress Table with Angio Arm Ergometer, Lode -927900, Holland) was used for exercise stage.

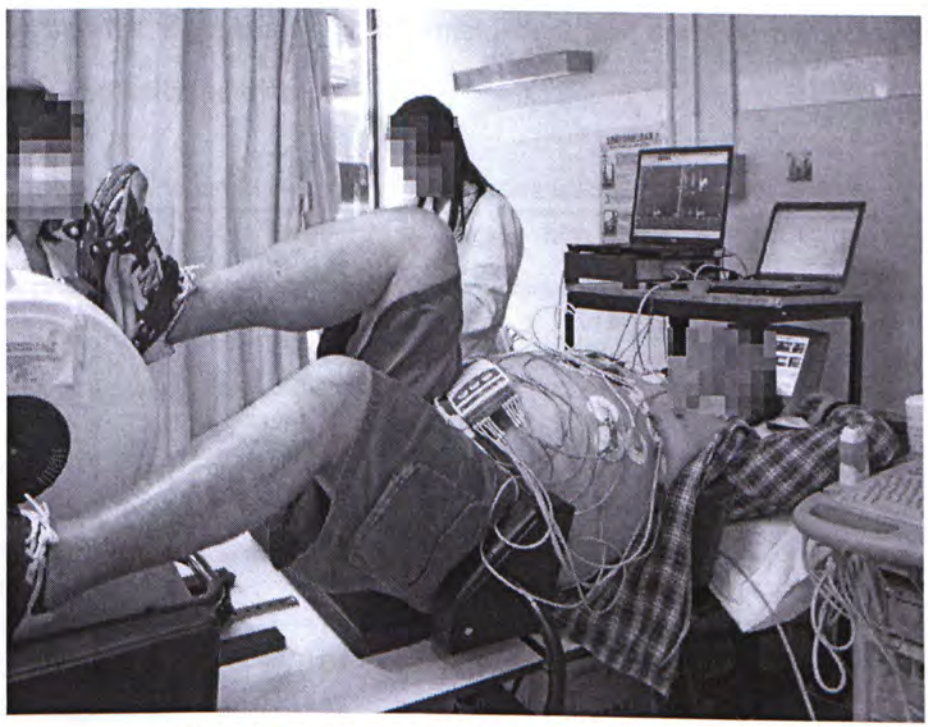

Fig. 5.2 Real view of experiment situation in PWH

During the experiment, subjects lay down on a special bed which can be manually rotated. The angle of bed for each subject was varied from 10° to 20° in order to get the clearest ultrasound imaging of heart. At the beginning of the experiment, each subject, with his right hand put on the side of his body and left hand on the pillows besides his head, was rest for 5~7 minutes, when at least two BP readings were

acquired. Then subjects began to cycle the bicycle under the supervision of doctors and nurses. The work load of bicycle was gradually increased from zero by 25w per 2 minutes and kept on a relative high level according to the physiological conditions of each subject. The length of exercise time was depended on whether the acceleration of heart rate was achieved at least 80% of the expected value. This target heart rate was decided in the previous diagnosis. Bicycle exercise was followed by a recovery stage lasting 10~15 minutes with subjects remaining at rest. In addition to the continuous physiological signal acquisition and intermittent BP measurement per two minutes, ultrasound images were achieved by a nurse from Princes of Wales Hospital during both exercise and recovery stages. Fig. 5.2 is a real photo taken in the hospital, showing the experiment situation when a subject was cycling

Table 5.1 lists the target heart rate, maximum work load during exercise and the time of exercise implemented by each subject.

Table 5.1 The target HR, maximum exercise load and durations of subjects

Subject No.	Target HR (beat / min)	Max. Load (w)	Exercise (min)
090227_1	154	75	19
090227_2	160	125	15
090227_3	137	70	16
090227_4	155	100	11
090306_1	149	100	15
090306_2	157	150	20
090313_1	170	100	18
090313_2	157	125	12
090313_3	171	100	14
090320_1	160	75	16
090320_2	149	75	15
090320_3	169	75	9
090320_4	159	75	10
090320_5	161	100	12
090320_6	171	120	22
090327_1	158	100	14
090327_2	167	100	16
090403_1	147	75	11
090403_2	150	75	12
090403_3	146	100	12

5.3. Data analysis

5.3.1. Partition of signal trials and selection of datasets

The recorded signal trials were uninterruptedly recorded for 18 minutes per subject in Experiment IV and ranging from 15 to 30 minutes in Experiment V. These trials should be divided into small segments for the convenience of further signal process. Therefore, according to the reference cuff BP readings, they were cut into two types of fragments. Fragments of Type I were cut from the time when the BP cuff began to be inflated while those of Type II were cut from the middle of every two cuff inflations. Each fragment was 40 seconds long and the remaining part after cutting was not used. Generally, a total of 300 datasets in Experiment IV and 556 datasets in Experiment V were collected.

However, the signal qualities in some datasets were not good enough for information extraction. Noise was introduced by motion artifact, external electromagnetic interference or hardware failure. Those noisy datasets, 41 trials in Experiment IV and 5 trials in Experiment V, were excluded from the dataset pool.

The reference BPs for datasets of Type I in Experiment IV were just those nurse readings coinstantaneous with signal recording; the references for Type II were the average values of nurse readings before and after each fragment. Since the nurse failed to hear the BP value once, 1 dataset of Type I and 2 datasets of Type II had no reference. In Experiment V, the references for Type I were the average of simultaneous auto-machine measurements and nurse readings when signals were recorded; the references for Type II were the average of simultaneous auto-machine measurements and nurse readings before and after signal recording. If the difference between auto-machine and nurse BP values was larger than 10 mmHg, then the reference BP was consider as unreliable reference. 94 references were judged and excluded as unreliable references, 30 out of which were excluded because of

emergency error of auto-machine during the experiment.

Finally, there were a total of 713 datasets selected for further analysis. Table 5.2 gives a detailed summary of dataset selection in both two experiments. Those selected datasets, including datasets at rest state, during exercise, and in recovery stage, were first processed by using the algorithm in section 4.2.2. Both PATs from ECG to finger PPG and ear PPG were calculated. It should be noted that the definition of ear PAT is the time division from ECG R-peak to the foot point of ear PPG, which is slightly different from the definition of finger PAT.

Table 5.2 Summary of dataset selection

	Experiment IV		Experiment V	
Total No. of datasets	300		556	
Signal length / dataset	40 second		40 second	
Types of BP ref.	Nurse readings		Nurse readings and auto-machine measurements	
Bad signal quality	5 datasets		41 datasets	
Ref. missing or unreliable	3 datasets		94 datasets	
No. of selected datasets	292		421	
	Rest	78	Rest	57
	Exercise	116	Exercise	206
	Recovery	98	Recovery	158

5.3.2. PPG waveform processing

PPG signal is sensitive to motion artifact, contact force variation and external light noise. In addition, the heart period variation may bring confusing information for intra-heart-period waveform analysis. In order to exclude all these negative influences, a noise reduction method mainly derived from time-domain periodic average method was used in these two experiments.

In the previous processing for PAT calculation, the foot, first derivative peak and maximum points of PPG signal have been characterized in time domain. According

to these characteristic points, the PPG signal in a trial can be cut into wave pieces from the foot point to the foot point and the amplitude of each wave can be defined as the voltage difference between the foot point and the maximum point. Secondly, waves having similar amplitudes (difference with the average amplitude was smaller than 20% of the average amplitude) were considered as stable waves less interfered by noises. Thirdly, those selected waves were rescaled to 2000 points per wave so that the time difference caused by heart rate variation was excluded. The linear interpolation method was used for resampling waves. Finally, the average of those resampled waves was treated as the representative waveform for a specific trial. Fig. 5.3 shows the procedures to process a typical PPG signal trial, amongst which the yellow line in Fig. 5.3(c) was the final averaged wave.

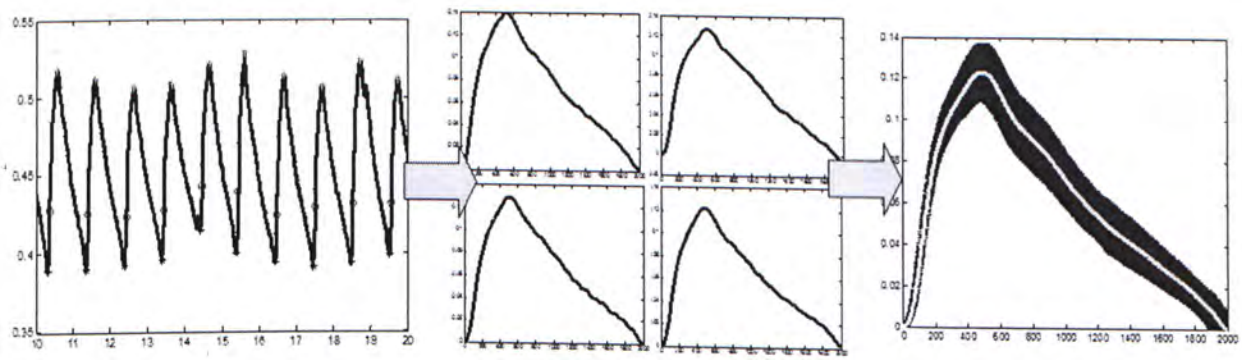

(a) (b) (c)

Fig. 5.3 Rescaling, resampling and superposition of PPG signal: (a) A typical trial of PPG signal with characteristic points; (b) rescaled wave pieces (2000 points per wave); (c) averaged wave of a trial signal (yellow line) and the SD of each point (blue shadow).

According to these averaged waves (PPG wave), first and second derivative PPG were derived and the waveform parameters proposed in Section 3.3.2 were calculated one by one.

5.4. Experiment results

5.4.1. Range and variation of reference SBP

Since a large amount of datasets including physiological state changes were collected on over 40 subjects, the systolic blood pressure covered a large area of values from 86 mmHg to 220 mmHg. The mean and standard deviation of SBP were 125.6±20.4 mmHg for young subjects (Experiment IV) and 159.6±27.4 mmHg for aged subjects (Experiment V). Fig. 5.4 shows the distribution of SBP values in both experiments. From the view of individual case, the SBP variations were averagely 12.1 mmHg for subjects in Experiment IV and 20.1 mmHg for subjects in Experiment V (Table 5.3).

Table 5.3 The standard deviation of SBP variation of each subject

Experiment IV		**Experiment V**	
Subject	**SD of SBP**	**Subject**	**SD of SBP**
e01	10.3	090227_1	26.6
e02	15.3	090227_2	27.1
e03	7.4	090227_3	12.6
e04	5.9	090227_4	10.3
e05	3.9	090306_1	20.6
e06	6.9	090306_2	21.6
e07	8.2	090313_1	21.5
e08	13.1	090313_2	25.9
e09	11.5	090313_3	27.6
e10	20.3	090320_1	20.1
e11	11.5	090320_2	24.1
e12	15.0	090320_3	16.0
e13	18.4	090320_4	14.1
e14	16.8	090320_5	17.1
e15	15.3	090320_6	31.9
e16	21.0	090327_1	19.8
e17	5.6	090327_2	14.6
e18	15.8	090403_1	16.9
e19	7.6	090403_2	22.6
e20	11.7	090403_3	30.7
Mean	**12.1**	**Mean**	**21.1**

Unit: mmHg

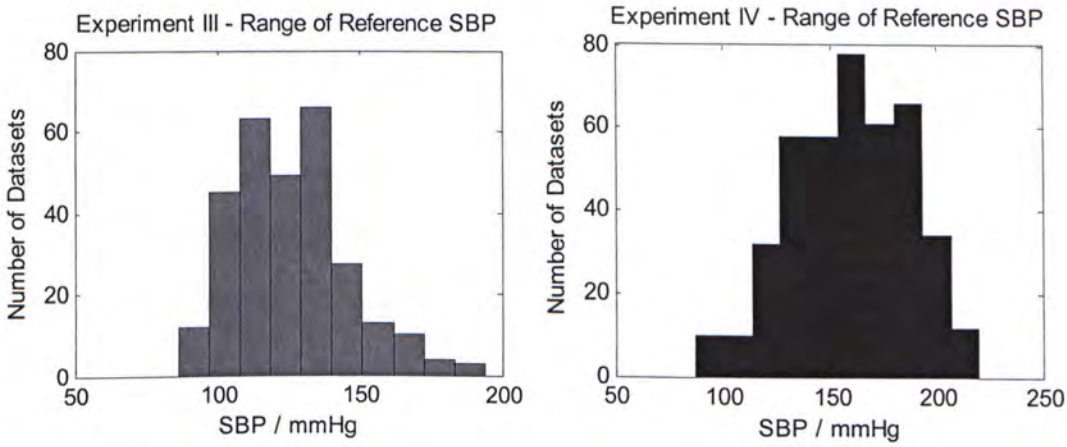

(a) (b)

Fig. 5.4 Distribution of SBP values: (a) in Experiment IV; (b) in Experiment V

5.4.2. PAT-BP individual best regression

Table 5.4 Individual standard deviation of errors of PAT-SBP regression

Subject	Using finger PAT	Using ear PAT	Subject	Using finger PAT	Using ear PAT
e01	4.3	5.3	090227_1	10.5	7.3
e02	7.6	6.7	090227_2	9.2	5.5
e03	5.1	6.2	090227_3	12.3	7.6
e04	3.8	4.8	090227_4	8.9	8.9
e05	2.9	3.3	090306_1	6.3	11.4
e06	5.1	5.6	090306_2	6.7	5.1
e07	4.3	5.6	090313_1	6.5	6.5
e08	7.3	7.4	090313_2	8.4	9.8
e09	6.1	7.2	090313_3	5.2	4.6
e10	5.5	9.8	090320_1	3.6	7
e11	6	6.7	090320_2	9	7.7
e12	7.6	9.7	090320_3	5.1	2.8
e13	6.6	8.2	090320_4	11.8	10.1
e14	4.9	8.3	090320_5	7.3	4.7
e15	9	8.3	090320_6	11	7.6
e16	7.4	10.3	090327_1	4	3.8
e17	4.6	5.6	090327_2	7	5.4
e18	11.5	11.1	090403_1	10.7	5.4
e19	6.1	5.7	090403_2	14.8	13.3
e20	8.4	7.5	090403_3	9.5	3.6
Overall	6.2	7.2	Overall	8.6	7.4

Unit: mmHg

Individual regression of SBP by PAT was achieved by using the Eq. 3.1 $SBP = A \cdot \ln(PAT) + B$. The RMSE of regression for each subject were varied from 2.9 mmHg to 14.8 mmHg and from 2.8 mmHg to 13.3 mmHg by using finger and ear PAT respectively. Detailed RMSE information of individual regression was listed in Table 5.4. Generally speaking, the RMSE of individual regression for young subjects were 6.2 mmHg for finger PAT and 7.2 mmHg for ear PAT. RMSE of regression for aged subjects were a little bit larger, which were 8.6 mmHg for finger PAT and 7.4 mmHg for ear PAT.

The following four figures (Fig. 5.5~Fig. 5.8) give some examples of best and worst cases of individual regression. The left sub-graph compares the estimation results with reference according to the time axis of data collection. And the right sub-graph shows the relationship between SBP and $\ln(PAT)$. In the best cases, PAT can sensitively track the changes of SBP, such as showed in Fig. 5.5 and Fig. 5.7, examples for Experiment IV and V respectively. However, as the worst cases, PAT had low correlations with SBP variations (Fig. 5.6 and Fig. 5.8).

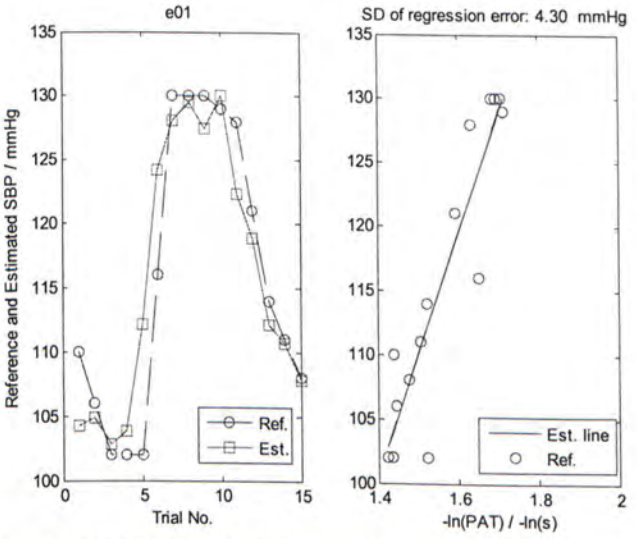

Fig. 5.5 Individual regression: example of best case in Experiment IV (finger PAT)

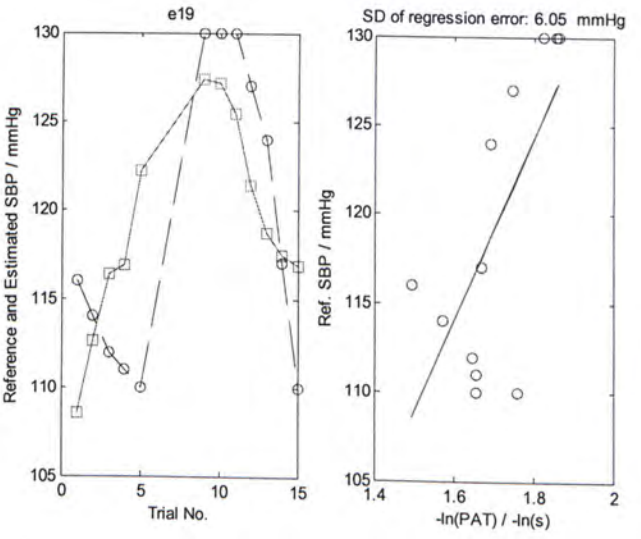

Fig. 5.6 Individual regression: example of worst case in Experiment IV (finger PAT)

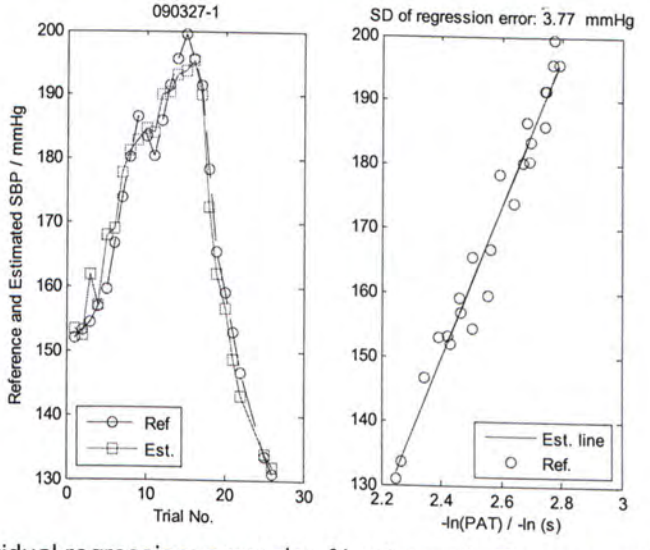

Fig. 5.7 Individual regression: example of best case in Experiment V (ear PAT)

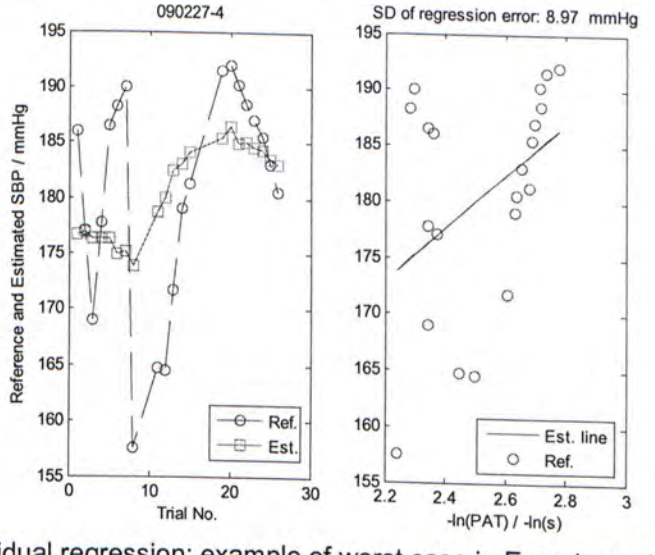

Fig. 5.8 Individual regression: example of worst case in Experiment V (ear PAT)

5.4.3. Multiple regression using ZX and arm length

According to the previous method of Eq. 3.8, if the SBPs were only regressed by finger PAT, the RMSEs of regression were 15.5 mmHg and 20.5 mmHg for Experiment IV (P-value of C_0>0.1 and C_3<0.001) and Experiment V (P-value of C_0>0.1 and C_3<0.001) respectively. If the SBPs were regressed by finger PAT, the length of arm and ZX, in experiment IV, the RMSE of regression was 13.4 mmHg with the P-values of C_0, C_2 and C_3 <0.001. However, the P-value of C_1 was larger than 0.1. In experiment V, the SD of regression error with three variables was 20.3 mmHg with the P-values of C_0<0.01, C_2<0.005, C_3<0.001 and C_1>0.1.

5.4.4. One-cuff calibration improved by PPG waveform parameter

Based upon the Eq. 3.9, an one-cuff individual calibration was purposed to be achieved with PAT and a PPG waveform parameter.

Table 5.5 Group correlation of SBP/age with PPG waveform parameters

	Reference SBP	Age of subjects
Reference of SBP		0.56
Age of subjects	0.56	
MaxP	**0.66**	**0.67**
L20	0.38	0.59
L40	0.37	0.61
L60	0.45	0.51
L80	0.49	0.41
DfrontP	0.29	0.24
DbackP	0.50	0.36
MaxV	-0.39	-0.66
DfrontV	**-0.45**	**-0.71**
DbackV	-0.38	-0.55
ZX	-0.22	-0.24
Hrate	0.33	0.10
Vrate	0.56	0.44
2ndD_area	0.15	-0.03

The group correlation between SBP/age and PPG waveform parameters: First of all, in order to select one of the 14 PPG waveform parameters proposed in Section 3.3.2 as the extra parameter used in PAT-BP estimation, the relationships among blood pressure, age and PPG waveform were investigated by group correlation. As calculated in Table 5.5, it is found that the parameter MaxP had a relative high correlation with both SBP (r=0.66) and age (r=0.67) while DfrontV had the highest correlation with age (r=0.71). Finally, MaxP was selected as the PPG waveform parameter used in Eq. 3.9.

Individual regression of SBP by PAT and MaxP: Individual regression of SBP was approached by using the equation

$$SBP = D_2 \cdot \ln(PAT) + D_1 \cdot MaxP + D_0, \qquad \text{Eq. 5.1}$$

amongst which finger PAT was used for young subjects, ear PAT for aged subjects and MaxP from finger PPG for all subjects. The overall RMSE of individual best regression was reduced from 7.0 mmHg to 6.2 mmHg (Table 5.6).

Table 5.6 Results of individual regression by Eq. 5.1

	PAT used	MaxP used	RMSE of individual regression	
			With only PAT	With PAT and MaxP
Experiment IV	Finger	Finger	6.2 mmHg	5.7 mmHg
Experiment V	Ear	Finger	7.4 mmHg	6.5 mmHg
Overall			7.0 mmHg	6.2 mmHg

SBP estimation with cuff BP calibration: Table 5.7 shows the comparison of estimation with and without MaxP by different calibration methods. As proposed in previous discussions in Chapter 3, the coefficients of D_1 and D_2 were set as group constants while D_0 was calculated by cuff BP readings. Two different sets of BP readings were used for comparison. For one-point calibration, only one cuff-BP reading at the rest stage was used for each subject, while another BP reading was included for the two-point calibration, where these two BPs had more than 20 mmHg

difference. In two-point calibration, the value of D_0 was determined as the average of the calculation results by the two readings. By using MaxP, the mean and standard deviation errors of estimation was reduced from 4.3±11.7 mmHg to -0.3±11.2 mmHg by one-point cuff calibration and further reduce to -1.4±9.9 mmHg by two-point calibration.

Table 5.7 Estimation results by Eq. 5.1 using cuff BP calibration

Cal. Points	Experiment IV		Experiment V		Overall	
	only PAT	PAT and MaxP	only PAT	PAT and MaxP	only PAT	PAT and MaxP
1 point at rest	2.7±12.4	-1.8±11.9	5.5±10.9	0.8±10.5	4.3±11.7	-0.3±11.2
2 points (BP range>20 mmHg)	4.4 ±9.7	-2.5±9.4	3.7±10.9	-0.5±10.3	3.0±10.4	-1.4±9.9

Unit: mmHg

5.5. Discussion

The large subject pool and the inclusion of bicycle exercise for dozens of minutes made the recorded SBP covering and varying in a large range in Experiment IV and V. The reference SBP range 86 mmHg~220 mmHg with a SD of 29.8 mmHg (Table 5.3) are much larger than it of any studies reviewed in Chapter 3. It is the proof of the success of experiment conduction but also brings more challenges to BP estimation.

PAT still has high individual correlations with SBP and the regressions of SBP by PAT for each subject had an overall error around 7 mmHg (Table 5.4). However, for every specific subject, the correlations between PAT and SBP are pretty high in some cases so that PAT can track SBP variation well (Fig. 5.5 and Fig. 5.7), while there are some bad situations that changes of PAT are definitely different from changes of SBP(Fig. 5.6 and Fig. 5.8). The worst cases happened in both young group and aged group but its reasons haven't been identified yet.

The cuffless calibration method invented in Chapter 4 still did not work well. According to the group regression results, it indicates that the arm length really has a

correlation with SBP because the coefficient P-values of the item of arm length are smaller than 0.005 for groups with different ages. However, the impact by ZX is not positive in supine position. Some physiological factors may disturbed the properties of ZX.

The cuff-based calibration method of Eq. 3.9 was used as an alternative choice. By comparing the group correlation with SBP and age, MaxP was selected as the representative of arterial elastic properties from all the 14 PPG waveform parameters proposed in Chapter 3. The estimation result with PAT and MaxP was improved from 4.3 ± 11.7 mmHg to -0.3 ± 11.2 mmHg by one cuff-BP calibration. Results for both young and aged group had been considerably better, indicating this method can be applied on different groups. Besides, the estimation results of MaxP calibration with one cuff BP are comparative to other cuff-based calibration mentioned in Section 3.2.1 (Table 5.8).

Table 5.8 The comparison among cuff-based calibration methods of PAT-BP estimation

Calibration approach	C. Poon's work (Section 3.2.1)	M. Wong's work (Section 3.2.1)	**Proposed cuff-based method**
Type of estimated BP	SBP	SBP	SBP
range of reference (mean±SD mmHg)	122±21	103.0±11.3	145.7±29.8
No. of subjects	85	14	40
Age of subjects (year)	57±29	26±4	45±19.5
Estimation error (Mean±SD mmHg)	0.6±9.8	5.8±4.2	-0.3±11.2
SD Ratio of Error to reference SBP (%)	46.7	37.2	37.6

In addition, the calibration using two cuff BP readings (difference >20 mmHg), can further improved the estimation result to -1.4 ± 9.9 mmHg, showing the potentials of PAT-BP estimation can pass the AAMI standards by using information from PPG waveform for calibration. Nevertheless it is not practical yet in normal application to make the blood pressure of a specific user vary larger than 20 mmHg for calibration procedures.

6. Conclusion

In this thesis, calibration methods for cuffless arterial blood pressure estimation by pulse arrival time are fully discussed and compared. The hemodynamic theories, especially the Bramwell-Hill's model and the volume-pressure relationship, are analyzed as the theoretical foundation of PAT-BP estimation. Based on these theories, the importance of pressure pulse transit distance and elastic properties of blood vessels is emphasized for PAT-BP calibration approaches.

A novel model-based PAT-BP estimation equation has been proposed upon above theories, introducing arm length and parameters from PPG waveform for calibration variables. It is a combination of meeting the theoretical requirements and agreeing with the practical experimental experiences. Moreover, both cuffless and cuff-based calibration approaches have been derived from this invented equation.

Referring to the cuffless calibration approach, a new parameter ZX from PPG waveform is first defined in this thesis and successfully used to improve the accuracy of PAT-BP estimation on thirty-three subjects. Compared this new cuffless calibration with other existing cuffless calibration methods, the proposed method not only has better estimation accuracy, but also is easier to be operated with strong evidences in agreeing with the theoretical models. The efficiency of this method has been verified in overtime and exercise experiments.

Nevertheless, this cuffless method does not perform ideally when the subject posture is changed from sitting position to supine position. The substitute cuff-based calibration upon the same theory equation has been investigated for the measurement in supine position. The estimation results on forty subjects

comparative to other cuff-based calibrations and show the potential of improving estimation accuracy.

For the future work, to understand the difference of physiological mechanisms of BP estimation in different postures and to connect measured PPG waveform with cardiovascular models will be the next-step topics in the PAT-BP estimation and calibration.